International Journal of Pharmaceutics 430 (2012) 1–17

Contents lists available at SciVerse ScienceDirect

International Journal of Pharmaceutics

journal homepage: www.elsevier.com/locate/ijpharm

Structural modifications of ^{99m}Tc-labelled bombesin-like peptides for optimizing pharmacokinetics in prostate tumor targeting

Christos C. Liolios[a,b,*], Eirini A. Fragogeorgi[a], Christos Zikos[a], George Loudos[c], Stavros Xanthopoulos[a], Penelope Bouziotis[a], Maria Paravatou-Petsotas[a], Evangelia Livaniou[a], Alexandra D. Varvarigou[a], Gregory B. Sivolapenko[b,*]

[a] Institute of Radioisotopes & Radiodiagnostic Products, NCSR "Demokritos", 15310 Athens, Greece
[b] Laboratory of Pharmacokinetics, Department of Pharmacy, University of Patras, 26504 Patras, Greece
[c] Deparment of Medical Instruments Technology, Technological Educational Institute, 12210 Athens, Greece

ARTICLE INFO

Article history:
Received 20 December 2011
Received in revised form 24 February 2012
Accepted 26 February 2012
Available online 10 March 2012

Keywords:
Bombesin
^{99m}Tc
Pharmacokinetics
Tumor targeting
Scintigraphy

ABSTRACT

Purpose: The main goal of the present study was to investigate the importance of the addition of a positively charged aa in the naturally occurring Bombesin (BN) peptide for its utilization as radiodiagnostic agent, taking into consideration the biodistribution profile, the pharmacokinetic characteristics and the tumor targeting ability.
Methods: Two BN-derivatives of the general structure [M-chelator]-(spacer)-BN(2–14)-NH_2, where M: ^{99m}Tc or $^{185/187}$Re, chelator: Gly-Gly-Cys-, spacer: -(arginine)$_3$-, **M-BN-A**; spacer: -(ornithine)$_3$-, **M-BN-O**; have been prepared and evaluated as tumor imaging agents.
Results: The peptides under study presented high radiolabelling efficiency (>98%), significant stability in human plasma (>60% intact radiolabelled peptide after 1 h incubation) and comparable receptor binding affinity with the standard [^{125}I-Tyr^4]-BN. Their internalization rates in the prostate cancer PC-3 cells differed, although the amount of internalized peptide was the same. The biodistribution and the dynamic γ-camera imaging studies in normal and PC-3 tumor-bearing SCID mice have shown significant tumor uptake, combined with fast blood clearance, through the urinary pathway.
Conclusion: The addition of the charged aa spacer in the BN structure was advantageous for biodistribution, pharmacokinetics and tumor targeting ability, because it reduced the upper abdominal radioactivity levels and increased tumor/normal tissue contrast ratios.

1. Introduction

Recently radiolabelled peptides have attracted considerable interest due to their wide applicability in the development of target-specific radiopharmaceuticals. They can easily be used as carriers for the delivery of radionuclides to tumors, infarcts, and infected tissues for diagnostic imaging, as well as for radiotherapy. Thus, many regulatory peptides are often under investigation to determine their potential application in the field of Nuclear Medicine (Reubi, 2003; Okarvi, 2004; Lee et al., 2010). One of the most promising peptides for scintigraphy of tumors over-expressing gastrin-releasing peptide receptors (GRPrs) is the tetradecapeptide bombesin (BN), (pGlu^1-Gln^2-Arg^3-Leu^4-Gly^5-Asn^6-Gln^7-Trp^8-Ala^9-Val^{10}-Gly^{11}-His^{12}-Leu^{13}-Met^{14}-NH_2), originally isolated from the skin of the Bombina frog (Anastasi et al., 1971, 1972). The receptors for the bombesin-like peptides are highly homologous seven-transmembrane, G-protein coupled receptors (Spindel, 2003; Smith et al., 2005; Jensen et al., 2008) known to get internalized after the receptor-agonist complex has been formed.

Several BN peptides labelled with ^{99m}Tc have already been evaluated for preclinical testing (Spindel, 2003) and clinical application in cancer detection (Van de Wiele et al., 2000, 2001a,b, 2008; Scopinaro et al., 2003, 2004; De Vincentis et al., 2004; Cantorias et al., 2007). ^{99m}Tc, which emits a single 140 keV gamma

Abbreviations: aa, amino acids; AUC, area under the curve of concentration versus time plot; AUMC, area under the fist moment curve; BN, bombesin; Boc, tert-butyloxycarbonyl; DCM, dichloromethane; DIC, N,N′-diisopropylcarbodiimide; DIEA, diisopropylethylamine; DMF, N,N′-dimethylformamide; Fmoc, 9-fluorenylmethoxycarbonyl; GRPrs, gastrin-releasing peptide receptors; HOBt, 1-hydroxybenzotriazole; ID, injected dose; Pbf, 2,2,4,6,7 – pentamethyldihydrobenzofuran-5-sulfonyl; p.i, post injection; MEK, Methyl Ethyl Ketone; MRT, mean residence time; ROI, region of interest; Rt, Retention time; SPPS, solid phase peptide synthesis; THF, tetrahydrofurane; Trf, triphenylmethyl; TFA, trifluoroacetic acid; $T_{1/2}$, half life decay time of the radionuclide.

* Corresponding authors at: Laboratory of Pharmacokinetics, Department of Pharmacy, University of Patras, 26504 Patras, Greece. Tel.: +30 2610 969816, fax: +30 2610 996302.
E-mail addresses: xliolios@upatras.gr (C.C. Liolios), gsivolap@upatras.gr (G.B. Sivolapenko).

0378-5173/$ – see front matter © 2012 Elsevier B.V. All rights reserved.
doi:10.1016/j.ijpharm.2012.02.049

ray ($T_{1/2}$ = 6.02 h), is an ideal radioisotope for SPECT imaging, since it is readily available from ^{99}Mo/^{99m}Tc generators, while its relatively short half-life allows scanning procedures, which collect data rapidly, but keep total patient radiation exposure low. The radiochemical characteristics of ^{99m}Tc are especially suitable for tumor-specific radiopharmaceuticals that have biological half-lives well-matching the time-course of tumor uptake and the background clearance of the radiolabelled, tumor-targeting biomolecules, e.g. BN-like peptides (Liu and Edwards, 1999; Seo et al., 2005).

Various approaches have been followed, aiming to provide easy, efficient and stable labelling of BN analogues with ^{99m}Tc. This is mainly accomplished by the covalent attachment of a bifunctional chelator, for the complexation of the $[Tc^{(V)}=O]^{3+}$ core (Wong et al., 1997; Lin et al., 2004, 2005; Blok et al., 2004; Van de Wiele et al., 2000, 2001a,b, 2008; Smith et al., 2003a,b, Trejtnar et al., 2000; Gourni et al., 2009; Fragogeorgi et al., 2009), or the tricarbonyl $[Tc^{(I)}(CO)_3]^+$ core (La Bella et al., 2002a,b; Smith et al., 2003a,b; Alves et al., 2006; Veerendra et al., 2006) to the targeting biomolecule with or without the presence of an intermediate linker/spacer chain.

Among the BN analogues studied, two basic structure types can be recognised: the first includes analogues, in which only a small portion of natural peptide sequence is retained, usually BN(7–14), with the addition of a chelator group and a spacer chain (Decristoforo and Mather, 2002; Rogers et al., 2003; Smith et al., 2003a,b; Giblin et al., 2005; Veerendra et al., 2006; Alves et al., 2006; Yang et al., 2006; Kunstler et al., 2007; Parry et al., 2007; Prasanphanich et al., 2007; Garayoa et al., 2007, 2008; Ananias et al., 2008; Schweinsberg et al., 2008; Lane et al., 2008; Gourni et al., 2009), while the second type includes analogues availing the full length of the BN peptide chain, with one or more amino acid residues of the N-terminal region being selectively replaced by a chelator group and/or a spacer chain (Baidoo et al., 1998; Breeman et al., 1999a,b; Chen et al., 2004; Lin et al., 2004, 2005; Yang et al., 2006; Fragogeorgi et al., 2009).

In general, the spacer technology seems to be one of the most promising proposals concerning the design of new BN analogues (Garayoa et al., 2008; Schweinsberg et al., 2008; Fragogeorgi et al., 2009; Lane et al., 2010) as well as of other bioactive peptides targeting G-protein coupled receptors (Kolenc-Peitl et al., 2011) that may be applied as radiodiagnostic/radiotherapeutic agents. The role of this spacer chain would be to prevent a possible interaction between the radiometal–chelator complex and the receptor binding region of the biomolecule, which might possibly deteriorate its biological integrity. Additionally, the spacer chain can also act as a pharmacokinetic modifier of the biomolecule. For the latter, various types of spacer chains containing charged (positively or negatively) or neutral amino acids have been utilized (Garayoa et al., 2008; Schweinsberg et al., 2008; Fragogeorgi et al., 2009) in an effort to reduce radioactivity accumulation in the abdominal region. High radioactivity accumulation in the abdominal region may significantly deteriorate the capacity of the labelled peptide to effectively image or to treat tumors or metastatic lesions in this area of the body, resulting in low tumor/normal organ ratios (Decristoforo and Mather, 2002; Smith et al., 2005; Giblin et al., 2005). Therefore for imaging of prostate cancer, hydrophilic BN derivatives are preferred to lipophilic ones, since they show low uptake in the hepatobiliary tract (Ananias et al., 2008).

In previous studies of our group, we had obtained very promising in vivo tumor targeting utilizing the full-length, C-terminally amidated BN(2–14) attached to a N_3S-type tripeptide chelator (Gly-Gly-Cys) via various spacer groups (Gourni et al., 2009; Fragogeorgi et al., 2009). Having established the tumor binding efficiency of the above full-length structure, we had investigated an analogue which contained the positively charged, non-natural aa spacer -(ornithine)$_3$- (**M-BN-O**, M: ^{99m}Tc or $^{185/187}$Re, Fig. 1) (Fragogeorgi et al., 2009). This analogue showed superior tumor uptake and faster clearance compared to similar analogues without a spacer or with a neutral one (Gourni et al., 2009; Fragogeorgi et al., 2009). In this study, we synthesized a full-length, C-terminally amidated BN(2–14) analogue, attached to the tripeptide chelator (Gly-Gly-Cys) via a positively charged but more polar, than the one used in the previous study, natural aa spacer -(arginine)$_3$- (positively charged at pH < 12.5) (**M-BN-A**, M = ^{99m}Tc or $^{185/187}$Re, Fig. 1). The aim is to investigate whether the presence of a positively charged and highly polar tripeptidic spacer is the decisive factor for optimally high body clearance, while retaining the tumor binding

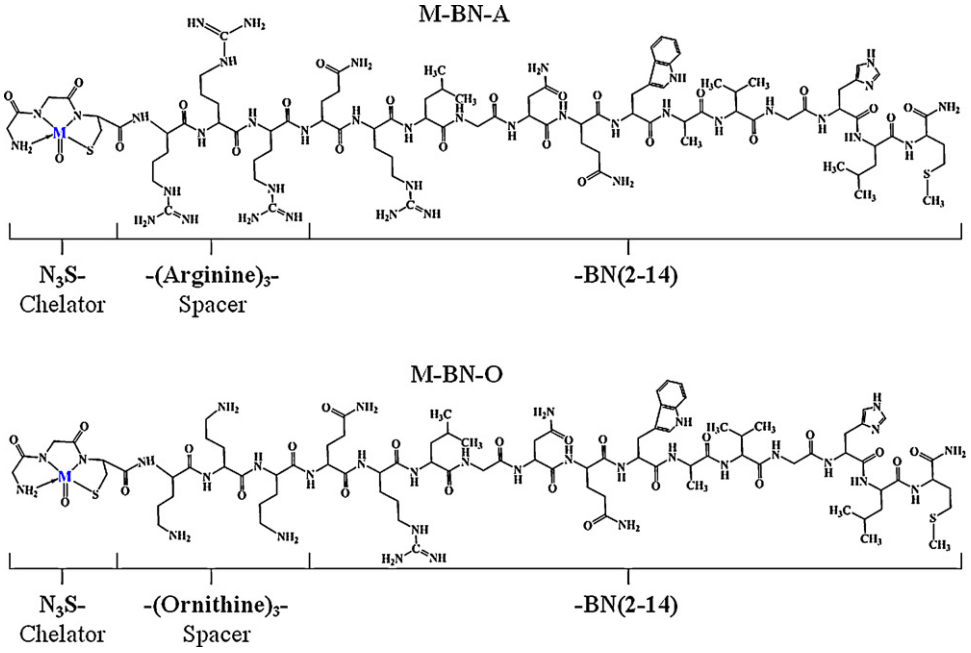

Fig. 1. Structure and amino acid sequences of **M-BN-A** and **M-BN-O**, where M = ^{99m}Tc or $^{185/187}$Re.

capacity. It is anticipated that this modification may lead to higher and earlier tumor binding with favorable tumor/non tumor ratios, while additionally a faster kidney clearance would limit kidney radioactivity exposure. The radiolabelling efficiency, the in vitro plasma stability, the prostate cancer cell binding, internalization and efflux, as well as the in vivo biodistribution and prostate tumor uptake in mice of **M-BN-A** were investigated and compared to the ones of **M-BN-O** (where M = ^{99m}Tc or $^{185/187}$Re).

2. Materials and methods

2.1. Materials

The Fmoc-protected amino acids were purchased from Merck/Novabiochem (Hohenbrunn, Germany). The side-chain protection groups of the amino acids were: Cys (Trt), Arg (Pbf), Orn (Boc), Trp (Boc), His (Trt). The polystyrene rink amide resin was purchased from Novabiochem. DMF, DCM, THF, TFA and CH_3CN (analytical grade) were obtained from Merck (Hohenbrunn, Germany) or Sigma–Aldrich (GmbH, Austria). All the other chemicals were obtained from Merck (Hohenbrunn, Germany). ^{99m}Tc, obtained in physiological saline as $Na^{99m}TcO_4$, was eluted from a commercial ^{99}Mo/^{99m}Tc generator (Mallinckrodt Medical, Petten, Netherlands). The human prostate adenocarcinoma cell line PC-3 was obtained from the American Type Culture Collection (ATCC). The product [^{125}I-Tyr^4]-BN was purchased from Perkin-Elmer (Life Science Products, Boston MA, USA, Inc.; specific activity, 81.4 TBq/mmol, 10 μCi). Biodistribution studies were performed using female normal Swiss and SCID (Severely Compromised ImmunoDeficient) mice (15–25 g) of the same colony and age, purchased from the Breeding Facilities of NCSR "Demokritos". Reagents and media for cell culture were purchased from PAA Laboratories GmbH (Austria) and all other chemicals from Merck (Hohenbrunn, Germany).

2.2. Instrumentation

Analytical Reverse Phase High Performance Liquid Chromatography (RP-HPLC) was performed on a Waters HPLC System (pump 616, UV detector 996 PDA) using a Hibar Pre-Packed Column RT 250-4, LiChrospher 100 RP-18 (5 μm) 250 mm, ID 4 mm, (Merck). Semi-preparative RP-HPLC was performed on a Waters (Milford, MA, USA) HPLC System (pump 600E, detector UV-484). A 10 Nucleosil 7 C18 column (250 mm × 12.7 mm ID, Macherey-Nagel, Dueren, Germany) was used. The HPLC analyses of radiolabelled peptides were performed on a Waters UV detector 996 PDA, Radioactivity detector γ-RAM, INSUS Systems, Inc. Mass spectra were recorded on an ESI Navigator Finnigan spectrometer. ESI-MS analysis was performed using the electrospray interface mass spectrometer Finnigan AQA Thermoquest. Instant Thin Layer Chromatography (ITLC) was developed on ITLC-SG (Gelman Sciences), while the measurements were performed with an electronic autoradiography system (Instant Imager Packard-Canberra). Gamma decay detection of ^{125}I for the in vitro cell binding studies was performed in a γ counter (Model LB2111, Berthold detection system, Bad Wildbad, Germany). For internalization, efflux and in vivo studies a multisample γ-counter system Packard Minaxi 5500 was used, equipped with a 3 in. NaI (Tl) crystal. Scintigraphic images were acquired by a dedicated small animal imaging system, based on 2 Position Sensitive Photomultiplier Tubes (Hamamatsu H8500); a pixilated NaI (Tl) scintillator with 1 cm × 1 cm × 5 cm 3 pixels and 0.2 mm pitch; a hexagonal parallel hole collimator with 1.5 mm diameter, 27.5 mm thickness and 0.25 mm septa. Eight position signals (2*X* and 2*Y* for each Photomultiplier) were transferred to a PC, equipped with 2 PCI6110 cards and controlled by Kmax software. The field of view of the system was 50 mm × 100 mm and spatial resolution equals 1.5 mm at 0 mm distance from collimators surface (Loudos et al., 2007).

2.3. Solid phase peptide synthesis

All the BN derivatives were synthesized manually on a Rink-amide resin employing the Fmoc strategy according to the literature (Kimmerlin and Seebach, 2005). In brief for coupling, an excess of the Fmoc-protected aa and HOB*t* were dissolved in *N*,*N*′-dimethylformamide (DMF). The solution was cooled on ice and then *N*,*N*′-diisopropylcarbodiimide (DIC) was added. The reaction mixture was initially left for 10 min in an ice bath and for another 10 min at room temperature and then it was added to the resin. The coupling efficiency was monitored by the Kaiser ninhydrin test (Sarin et al., 1981). Removal of the N-terminal Fmoc group was achieved by repetitive treatment with 20% piperidine in DMF. The final product was cleaved from the resin using a cocktail of trifluoroacetic acid (TFA), thioanisol, ethanediol, phenol, H_2O and triisopropylsilane (81.5/5/2.5/5/5/1, v/v/v/v/v/v). The crude product, obtained by precipitation with cold diethylether, was purified by semi-preparative RP-HPLC. Elution was performed with a solvent system consisting of 0.05% TFA in water (solvent A) and 60% CH_3CN in solvent A (solvent B), by applying a linear gradient from 100% to 40% solvent A in 47 min. The flow rate was 3.0 ml/min and the peptide peaks were detected with a UV detector at 220 nm.

2.4. Preparation of $^{185/187}$Re-BN derivatives (non-radioactive complexes)

The $^{185/187}$Re-BN derivatives were prepared by ligand exchange reactions, starting from the preformed $^{185/187}Re^{(V)}O$ gluconate precursor (Noll et al., 1996). An aqueous solution of both crude BN derivatives and a $^{185/187}Re^{(V)}O$ gluconate solution were allowed to react at 67 °C for 2 h. The crude $^{185/187}$Re-BN complexes were purified by semi-preparative RP-HPLC. Elution was performed with a solvent system consisting of 0.05% TFA in water (solvent A) and 60% CH_3CN in solvent A (solvent B), by applying a linear gradient from 100% to 50% solvent A in 50 min. The flow rate was 3.0 ml/min and the peptide peaks were detected with a UV detector at 220 nm. The pure $^{185/187}$Re-BN complexes were analysed by an analytical RP-HPLC, in comparison to the peptide conjugates, before and after the complexation reaction. Elution was performed by applying a linear gradient system from 100% to 50% solvent A in 25 min (Solvent system: solvent A: 0.05% TFA in a 0.1 M NaCl water solution and solvent B: 90%, 0.05% TFA/CH_3CN, 10%, 0.05% TFA in water). The pure $^{185/187}$Re-BN complexes were also characterized by ESI-MS.

2.5. Preparation of ^{99m}Tc-BN derivatives (radioactive complexes)

Radiolabelling of the BN derivatives was performed by radioisotope exchange from a $^{99m}Tc^{(V)}O$ gluconate precursor (sodium gluconate being used as an intermediate exchange ligand for ^{99m}Tc, with stannous chloride as the reducing agent) (Fragogeorgi et al., 2009). Thus, a solid mixture containing 1.0 g sodium gluconate ($C_6H_{11}NaO_7$), 2.0 g sodium bicarbonate ($NaHCO_3$) and 15 mg stannous chloride ($SnCl_2$) was homogenized and kept dry. 3.0 mg of the above mixture were dissolved in 1.0 ml of a sodium pertechnetate solution ($Na^{99m}TcO_4$), containing 370–555 MBq (10–15 mCi) of ^{99m}Tc and was left to react for 10 min at room temperature. An aliquot of 200 μl (2–3 mCi) of the above solution was added to 100 μl of an aqueous solution (pH 1–2) containing 10 μg of each BN derivative. The mixture (pH 6–7) was homogenized by vortexing and was allowed to react at 45 °C for 30 min.

2.6. Radiochemical analysis

The radio labelling yield and the stability of the radiolabelled products were determined by analytical RP-HPLC and by Paper Chromatography (ITLC-SG). RP-HPLC elution was performed with a solvent system consisting of: 0.1% TFA in water (solvent A) and 0.1% TFA in methanol (solvent B), by applying the following gradient: from 0% to 80% solvent B (1–20 min), 80% solvent B (20–23 min), 80–0% solvent B (23–25 min) and 0% solvent B (25–30 min) at a flow rate of 1.0 ml/min. The eluent was passed through a UV detector at 220 nm and through a sodium iodide scintillation detector, both connected to a computer for data analysis and storage.

The $^{99m}Tc^{(V)}O$ gluconate (^{99m}Tc-GL) precursor and the radioactive BN derivatives were also analysed by ITLC, on Silica Gel (ITLC-SG) strips. Briefly, 5 μl of the reaction mixtures were applied on three different strips (12 cm × 1 cm) of SG paper (application point: 2 cm from the bottom). The radiochromatographs were developed in saline (0.9% NaCl), acetone or MEK and Pyridine/CH_3COOH/H_2O (50/30/15) as a mobile phase over a distance of 10 cm. After drying the strips, their radioactivity was measured by electronic autoradiography. When normal saline was used, free $^{99m}TcO_4^-$ and ^{99m}Tc-GL migrate with the solvent front (Rf = 1.0), while peptide-bound ^{99m}Tc and colloid remain at the application point (Rf = 0.0). In acetone, free $^{99m}TcO_4^-$ migrates with the solvent front (Rf = 1.0), while ^{99m}Tc-GL, peptide-bound ^{99m}Tc and colloids remain at the spot (Rf = 0.0). In Pyridine/CH_3COOH/H_2O (50/30/15) (IAEA-TECDOC-1214, 1995–1999) everything but the colloids (Rf = 0.0–0.3) migrate with the solvent front (Rf = 1.0).

2.7. Metabolic stability in mouse and human plasma

Metabolic stability of the radiolabelled BN derivatives was studied in mouse and in human plasma. For mouse plasma a blood sample was collected from normal Swiss mice by cardiac puncture in heparinized polypropylene tubes, centrifuged at 6000 × *g* (4 °C) for 30 min and the supernatant (plasma) was isolated. For human plasma stability studies a blood sample was collected from healthy donors in heparinized polypropylene tubes, centrifuged at 2240 × *g* (4 °C) for 10 min and the supernatant (plasma) was collected. 50 μl (7.4–14.8 MBq or 200–400 μCi) of each radiolabelled BN derivative were incubated with 450 μl plasma at 37 °C. Fractions of 100 μl were withdrawn at 5, 15, 30 and 60 min. The proteins were precipitated with the addition of ethanol (2:1 EtOH/aliquot, v/v) (Fragogeorgi et al., 2009), and samples were centrifuged at 15,000 × *g* at 4 °C for 10 min. The supernatants were filtered through a filter (0.22 μm, Millipore GV) and analysed with RP-HPLC as described above. Recovery of radioactivity in the supernatant was 50–70%.

2.8. Cell culture

Human androgen-independent prostate cancer cells PC-3 were grown in DMEM Glutamax-I, supplemented with 10% (v/v) fetal bovine serum (FBS), 1% L-glutamine and 1% penicillin/streptomycin. Cells were incubated in a controlled humidified atmosphere containing 5% CO_2 at 37 °C and were subcultured weekly after being detached from the flask surface by trypsin/EDTA solution (0.25%).

2.8.1. In vitro cell binding studies

The IC_{50} values of the BN derivatives were assessed by a competitive cell binding assay utilizing [^{125}I-Tyr^4]-BN as the GRPr specific radioligand and [Tyr^4]-BN as a control compound. PC-3 cells suspended in medium, containing 1% FBS, 0.125% BSA, 0.25 mM PMSF, 1 μg/ml aprotinin and 50 μg/ml bacitracin, were distributed in 24-well plates and incubated at 37 °C for 1 h in the presence of 25000 cpm [^{125}I-Tyr^4]-BN (2200 Ci/mmol) and increasing concentrations of each BN derivative or its complex with non-radioactive $^{185/187}$Re, ranging from 10^{-12} to 10^{-6} M. In this assay [Tyr^4]-BN (in house-synthesized) was used as the control peptide. After incubation, the cells were washed twice with cold wash buffer and lysed with 1N NaOH. Radioactivity bound to the cells was counted in a γ-counter. Experiments were carried out three times in duplicate. IC_{50} values were calculated by non-linear regression analysis, using GraphPad Software (San Diego, CA, USA) Prism 4 computer fitting program.

2.8.2. Internalization and efflux analysis

The PC-3 cell line was used for the in vitro internalization and externalization assays of the BN derivatives. In detail, for the internalization assay the PC-3 cells were distributed overnight in six-well plates ($1.0–1.5 \times 10^6$ cells per well) at 37 °C in a 5% CO_2 air atmosphere in culture medium (DMEM with 10% FBS, L-glutamine and 1% penicillin/streptomycin). On the day of the experiment, the medium was removed and the cells were washed twice with cold buffer and were incubated in 1.2 ml internalization medium (DMEM containing 1% FBS) in the presence of 100,000–300,000 cpm of each ^{99m}Tc radiolabelled BN derivative (in 150 μl 0.5% BSA/PBS buffer corresponding to ~200 fmol total peptide) at 37 °C for 5, 15, 30, 60, 120 and 180 min. Specificity of internalization was evaluated in the presence of 1 μM unlabelled native BN (in house-synthesized). Upon completion of the incubation, cells were washed twice with cold PBS to discard unbound peptide. Surface-bound radioactivity was removed by washing the cells twice, for 5 min each time, with an acid solution (50 mM glycine, 0.1 M NaCl, pH 2.8). The amount of internalized peptides was recovered by solubilising the cells with 1N NaOH at 37 °C. The internalized radioactivity (% of total added), was determined using a multi-sample γ-counter.

The externalization studies were performed with additional incubation of the PC-3 cells in peptide-free medium after the maximum amount of internalization (plateau) was achieved. In detail, when the maximum internalization rates of the radiolabelled peptides were reached, the medium was discarded and the cells were washed three times with cold buffer. New medium was added and the cells were incubated at 37 °C. Sampling at 0, 15, 30, 60 and 120 min post-internalization was performed by an initial cold buffer wash of the cells, followed by acid wash (for removal of surface bound radioactivity), as previously described and finally by treatment with 1N NaOH to extract the radioactivity remaining trapped in the cells. Radioactivity was measured using a multi-sample γ-counter.

Results for both the above assays were expressed as the mean of 3 experiments ±SD, each performed in triplicate where each time point represents the percentage of the total cell bound radioactivity. A curve fitting was performed using the GraphPad software, where the "One Phase Association" and the "Dissociation–One phase exponential decay" equations were used for the internalization and externalization experiments respectively.

2.9. Biodistribution analysis

2.9.1. Normal Swiss mice

The in vivo behaviour was studied in normal female Swiss mice (average weight 20 ± 2.0 g) by injecting 100 μl, (125 ng, 0.075–0.125 mCi) of each radiolabelled BN derivative diluted in saline (pH 7), via the tail vein. Animals were sacrificed at predetermined time intervals of 5, 15, 30, 60, 90 and 120 min post injection (p.i.) and the main organs were removed, weighed and counted, together with samples of blood, muscle and urine, in a γ-counter. In reference to a standard of the injected solution, results were expressed as a percentage of the injected dose (% ID) per

organ and per gram of each organ or tissue. For total blood radioactivity calculation, blood is assumed to be 7% of the total body weight. Receptor blocking studies were also carried out with co-administration of an excess amount (100 μl, 1 mg/ml) of native BN. Animals were sacrificed 30 min p.i. and the tissues were removed, weighed and counted as previously described. In vivo studies were performed in compliance with the European legislation for animal welfare. All animal protocols have been approved by the Hellenic Authorities.

2.9.2. PC-3 tumor-bearing SCID mice

For the implantation of tumors, PC-3 cells freshly suspended in medium were subcutaneously injected in the left or right flank at a concentration of 10^7 cells/animal. Tumors were allowed to grow for two to three weeks. Animals were fed with autoclaved rodent food and water ad libitum, before and during the time of tumor growth. On the day of assay the mice (average weight 20 ± 2.0 g) were injected via the tail vein with 100 μl of a solution of **^{99m}Tc-BN-A** (0.075–0.125 mCi corresponding to 125 ng of total peptide) in saline (pH 7.0) and were sacrificed at 15, 30, 60 and 120 min p.i. For the determination of non-specific uptake, blocking experiments were performed, in which three mice received excess amount of native BN (100 μl, 1 mg/ml) along with the **^{99m}Tc-BN-A** and sacrificed at 30 min p.i.

2.10. Pharmacokinetic analysis

The mean of 3–4 animal concentration data (% ID/g) over time in normal mice was used for pharmacokinetic modelling. An intravenous bolus administration approach was applied to model the time concentration data and to estimate the elimination rate constants. The one and two compartment model approaches were used to fit the data of blood concentration with time. Selection of models was based on the F-test and the Akaike Information Criterion (statistical analysis data for model selection are included in supplementary material). The ^{99m}Tc-BN analogue blood concentration C^0 was calculated by projection of the previously mentioned model for $t = 0$ min. A non-compartmental analysis was followed for the rest of the organs in order to estimate the Area Under the Curve (AUC), the Area Under the first Moment Curve (AUMC), and the Mean Residence Time (MRT = AUMC/AUC). Clearance was calculated by the ratio CL = ID/AUC (ID = 100% of the injected dose).

2.11. Dynamic γ-camera imaging

Evaluation of the **^{99m}Tc-BN-A** was performed by dynamic imaging studies using a high resolution dedicated small animal γ-camera. PC-3 tumor-bearing SCID mice were anaesthetized with 100 μl of 10% xylazine and 5% ketamine (10 mg/kg mouse body weight) prior to scanning and positioned to the animal bed. 100 μl of approximately 7.4 MBq (~0.2 mCi) of **^{99m}Tc-BN-A** were administered through the tail-vein prior to anaesthesia. Static 2 min images were obtained for 120 min p.i. For the quantification of the obtained results all successive images were added, to provide a "summed" image with good statistics. On this image regions of interest (ROIs) were drawn on the tumor and several organs. In addition, a ROI that contains the entire mouse was used in order to allow the calculation of the percentage of total radioactivity in each organ. Data were corrected for ^{99m}Tc decay.

2.12. Statistical data analysis

All data were expressed as the mean of values ± standard deviation (mean ± SD). Data comparison was performed by using the Student's *t*-test. $P < 0.05$ was considered significantly different. The results from the IC_{50} in vitro cell assay were presented as mean ± standard error of mean (SEM). For their statistical evaluation one-way ANOVA was performed using GraphPad Software (San Diego, CA, USA) Prism 4 computer program, where differences at 95% confidence interval ($P < 0.05$) were considered significant.

3. Results

3.1. Synthesis and characterization

The synthesis of all the BN derivatives (Fig. 1) was performed following an Fmoc-based SPPS protocol. The crude products were purified by semi-preparative RP-HPLC. The chemical purity of the final products was above 95%, as determined by analytical RP-HPLC. Pure **BN-A** was obtained at a satisfactory yield, of about 39%; while on the other hand the introduction of the -(ornithine)$_3$- spacer in **BN-O** led to a significant reduction in the yield (~9%). The two peptides presented a retention time (Rt) difference of 1.8 min in the RP-HPLC analysis, with **BN-O** eluting earlier than **BN-A** (Fig. 2). Both derivatives were characterized with ESI-MS. The ESI-MS results along with the theoretically expected charged ion values and calculated MW are summarized in Table 1.

3.2. Preparation of $^{185/187}$Re-BN derivatives (non-radioactive complexes)

The non-radioactive $^{185/187}$Re complexes of **BN-A** and **BN-O** (Fig. 1), were synthesized via the $^{185/187}Re^{(V)}O$-gluconate precursor, purified by semi-preparative RP-HPLC and characterized by ESI-MS (Table 1). Complexation with $^{185/187}$Re resulted in a slight increase in their retention time (Rt) and their maximum UV absorbance during the RP-HPLC analysis (Fig. 2).

3.3. Radiolabelling-radiochemical analysis

Radiolabelling of the two new BN derivatives with ^{99m}Tc was performed by the preconjugation approach using the $Tc^{(V)}O$ gluconate precursor, as an intermediate exchange ligand. A two-strip ITLC-SG method for the analysis of precursor showed that no amount of either pertechnetate $^{99m}TcO_4^-$ or of colloidal ^{99m}Tc was present. The radiochemical yield for both BN derivatives was higher than 98%, providing a single radioactive species, as detected by both RP-HPLC and Paper Chromatography (ITLC-SG). The stability of the new radiopeptides, tested up to 6.0 h post-labelling, remained high (>90%). The Rt of both BN $^{185/187}$Re-derivatives, compared to those of their respective ^{99m}Tc-radioactive complexes, were similar after their co-injection into RP-HPLC, confirming that $^{185/187}$Re and ^{99m}Tc form complexes of similar structure (Fig. 2). During the RP-HPLC analysis, **^{99m}Tc-BN-O** was eluted earlier than **^{99m}Tc-BN-A** (Fig. 2).

3.4. Metabolic stability in plasma

3.4.1. Mouse plasma

The radio RP-HPLC analyses after the incubation of **^{99m}Tc-BN-A** and **^{99m}Tc-BN-O** in mouse plasma are reported in Fig. 3. After 5 min of incubation 42.48 ± 1.45 of **^{99m}Tc-BN-A** and 44.28 ± 3.84% of **^{99m}Tc-BN-O** remained intact. Both peptides presented similar metabolic patterns. One major radioactive metabolite (M) was present with Rt close to that of the intact peptide. This major metabolite (M-A for **^{99m}Tc-BN-A** and M-O for **^{99m}Tc-BN-O**) probably contained a great part of the parent peptide chain, including the chelator group still conjugated to ^{99m}Tc; further research is necessary in order to identify the extent of the parental peptide chain catabolism. Additionally, after 1 h incubation ~15% **^{99m}Tc-BN-A** and ~18% of **^{99m}Tc-BN-O** still remained intact, as shown by

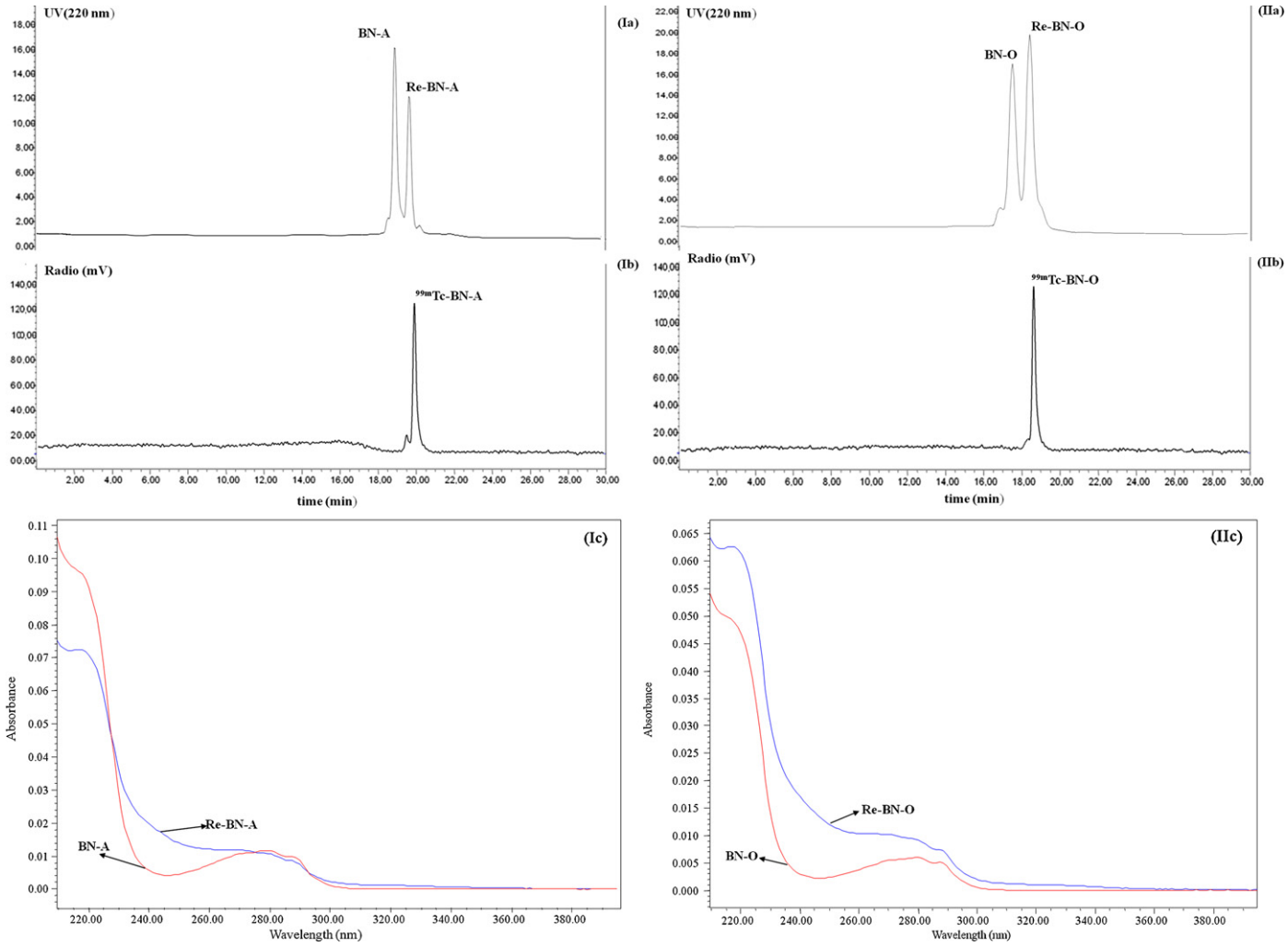

Fig. 2. RP-HPLC analysis of the two BN analogues co-injected (1:1 w/w) with their $^{185/187}$Re complexes (Ia, IIa); their ^{99m}Tc complexes (Ib, IIb); the UV-spectra of the BN analogues and their $^{185/187}$Re complexes, (Ic, IIc).

Table 1
Data for BN peptides and their $^{185/187}Re^{(V)}O$ complexes from ESI-MS analysis.

Compound	Calculated MW	Charged ion (m/z)	Theoretical value	Experimental value
BN-O	2068.4	$[M+2H]^{2+}$	1035.3	1035.0
		$[M+3H]^{3+}$	690.5	690.6
$^{185/187}$Re-BN-O	2267.6	$[M+2H]^{2+}$	1134.8	1134.7
		$[M+3H]^{3+}$	756.9	756.8
BN-A	2194.5	$[M+2H]^{2+}$	1098.2	1098.2
		$[M+3H]^{3+}$	732.5	732.6
$^{185/187}$Re-BN-A	2393.7	$[M+2H]^{2+}$	1197.8	1197.8
		$[M+3H]^{3+}$	798.9	799.4

the RP-HPLC analysis. In conclusion **^{99m}Tc-BN-O** proved slightly more resistant to the catabolic action of peptidases, while also the formation of the major metabolite (M-O) was slower.

3.4.2. Human plasma

The radio RP-HPLC analysis results after 1 h of incubation in human plasma of the ^{99m}Tc-BN derivatives are presented in Fig. 4. Over 60% of both tested radiolabelled BN derivatives remained intact (60.2 ± 1.2% for **^{99m}Tc-BN-A** and 63.0 ± 1.0% for **^{99m}Tc-BN-O**). Alike the mouse plasma analysis **^{99m}Tc-BN-O** proved slightly more resistant to degradation than **^{99m}Tc-BN-A**. The metabolic patterns observed for human plasma were similar with the ones observed in mouse plasma, although peptide degradation in human plasma was much slower. A radioactive metabolite with Rt close to that of the intact peptide (H) was also present, but in lesser amounts in comparison to the mouse plasma. This metabolite (M) while clearly visible for mouse plasma after the first 5 min of incubation, for the human plasma (H) it was visible only after 1 h of incubation. The amounts of (H) after 1 h of incubation were similar for both peptides (~4–5%).

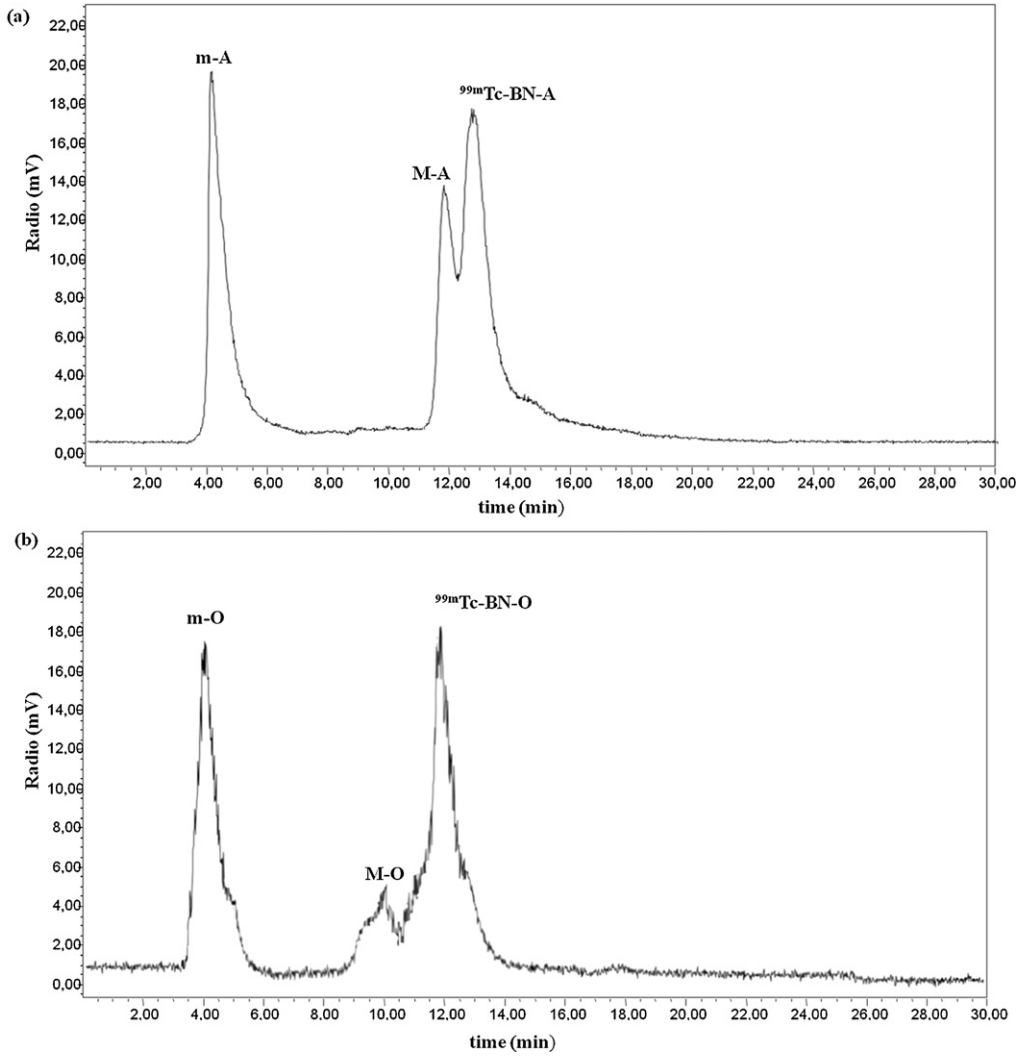

Fig. 3. RP-HPLC radioactivity detector analysis after 5 min incubation in mouse plasma of **^{99m}Tc-BN-A** (a) and **^{99m}Tc-BN-O** (b); M-A, M-O, major radioactive metabolites in mouse plasma for **^{99m}Tc-BN-A** and **^{99m}Tc-BN-O** respectively, m-A, m-O, ^{99m}Tc-radioactive degradation products of high polarity.

3.5. In vitro cell binding assays

The binding affinity of **BN-A** and **BN-O** and of their $^{185/187}$Re complexes for the GRPr was evaluated in the PC-3 cell line. A typical sigmoid curve for displacement of [^{125}I-Tyr^4]-BN from PC-3 cells, as a function of increasing concentration of all five different cold ligands studied (i.e. **[Tyr^4]-BN, BN-A, BN-O, $^{185/187}$Re-BN-A, $^{185/187}$Re-BN-O**), was obtained (Fig. 5). The determined IC_{50} values are summarized in Table 2. All the compounds exhibited affinity values similar to that of the control peptide [Tyr^4]-BN. The addition of the positively charged amino acid spacer and the Gly-Gly-Cys chelator group did not affect the binding affinity of the BN derivatives, while their complexation with Rhenium resulted in a marginally significant deterioration in affinity. The differences between the receptor affinities of **BN-A** and **BN-O**, as well as between their $^{185/187}$Re complexes were insignificant.

Table 2
The IC_{50} values of the tested BN analogues expressed in nM. Significantly different statistically from [Tyr^4]-BN according to the *t*-test (confidence interval 95%) are reposted as Y, and the not statistically significant as N.

Compound	IC_{50} (expressed in nM)	Std. Error	Statistically significant different from [Tyr^4]-BN
BN-A	0.50	0.09	N
$^{185/187}$Re-BN-A	1.58	0.16	Y
BN-O	0.46	0.04	N
$^{185/187}$Re-BN-O	0.77	0.07	Y
[Tyr^4]-BN	0.45	0.04	–

3.6. Internalization and efflux analysis

The uptake (internalization) and efflux (externalization), as a function of time of the radiolabelled BN derivatives under study, was assessed in a PC-3 cell line, in the presence (blocking experiments) or absence of native BN. The results of this study for **^{99m}Tc-BN-A** are reported in Fig. 6. The results for **^{99m}Tc-BN-O**, which was used as a reference for both assays, were similar with the ones previously reported by Fragogeorgi et al., 2009 (data not shown). The rate of internalized radioactivity of **^{99m}Tc-BN-A** was rapidly increased until 120 min after the initialization of its incubation with the PC-3 cell line. Between 90 and 120 min it reached a plateau, where it remained stable even after 3 h of incubation. Nonspecific internalization in the presence of native BN was lower than 5% and rather stable during the whole experiment. Comparing the above results with those previously reported for **^{99m}Tc-BN-O** (Fragogeorgi et al., 2009) we observed that **^{99m}Tc-BN-A** needed more time to reach the maximum of its internalization (plateau),

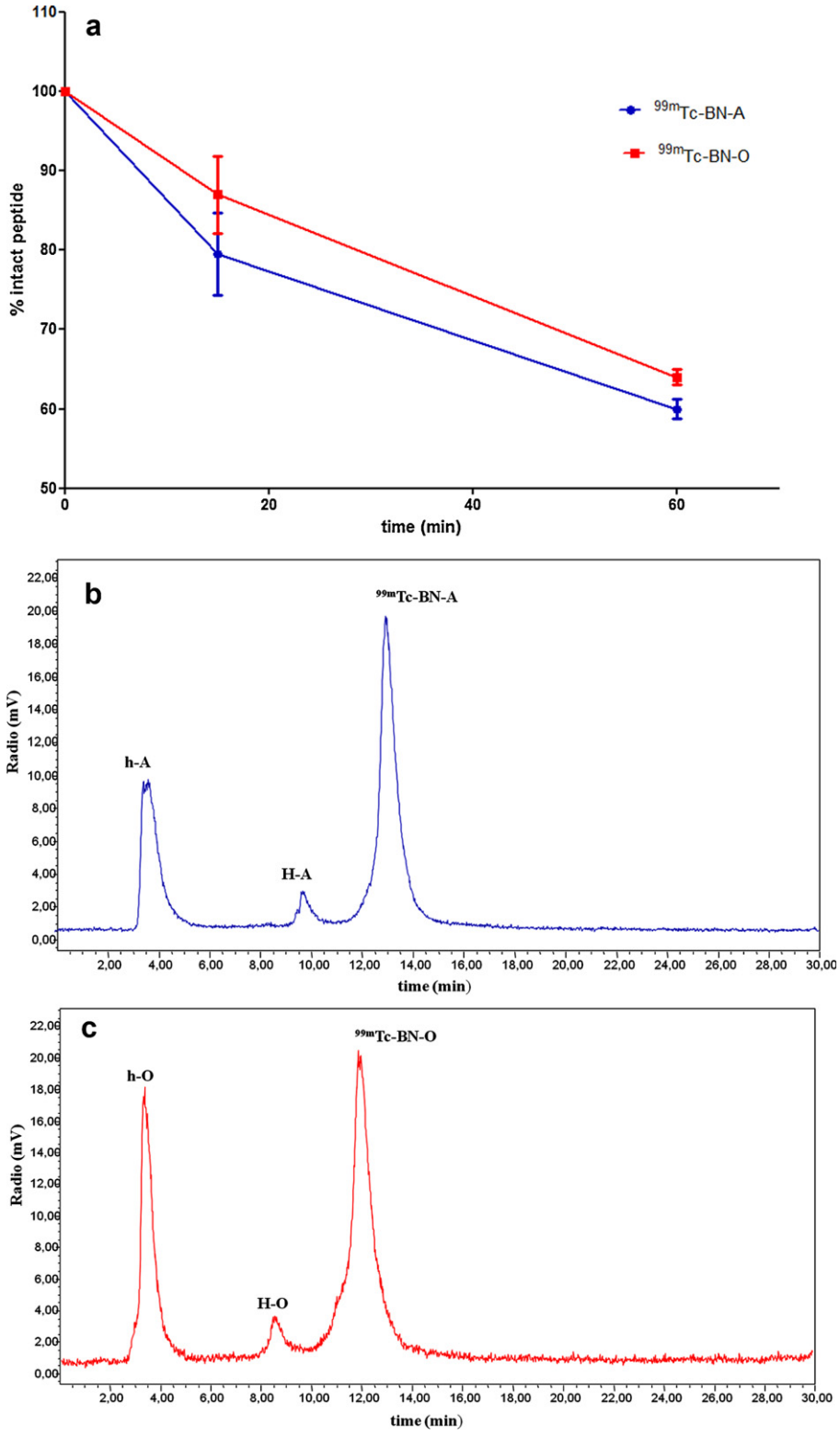

Fig. 4. Human plasma stability vs time for the two ^{99m}Tc-BN derivatives (a). RP-HPLC radio activity detector analysis after 1 h incubation in human plasma of **^{99m}Tc-BN-A** (b) and **^{99m}Tc-BN-O** (c); H-A, H-O, major radioactive metabolite in human plasma for **^{99m}Tc-BN-A** and **^{99m}Tc-BN-O** respectively; h-A, h-O, ^{99m}Tc-radioactive degradation products of high polarity.

which is indicative of a lower agonistic activity. More specifically, **^{99m}Tc-BN-O** reached its plateau after the first 60 min of its incubation. The specific and nonspecific (in the presence of native BN) internalization levels were the same for both peptides.

In order to evaluate the externalization rate, when **^{99m}Tc-BN-A** reached the maximum levels of its internalization (120 min), the PC-3 cell line was washed with acid buffer (removal of surface-bound activity) and then it was further incubated in fresh medium.

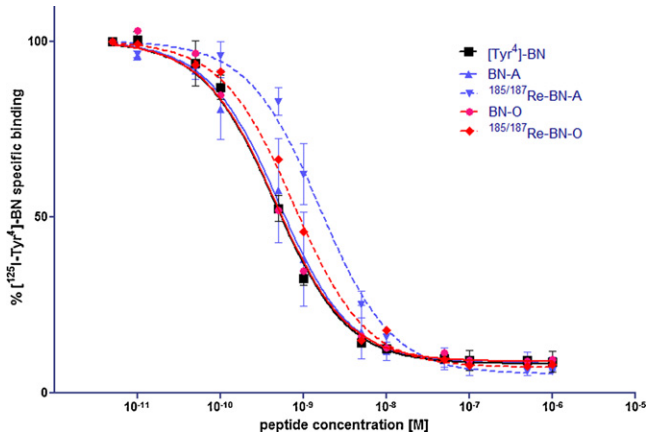

Fig. 5. Displacement curves of [^{125}I-Tyr^4]-BN bound to the GRPrs of PC-3 cells by: [Tyr^4]-BN (■, —), BN-A (▲, —), $^{185/187}$Re-BN-A (▼, - - -), BN-O (●, —), $^{185/187}$Re-BN-O (♦, - - -).

Measurements up to 90 min post-incubation showed that about 68% of **^{99m}Tc-BN-A** remained trapped into the cells (Fig. 6), a percentage similar to that obtained with **^{99m}Tc-BN-O**, indicative of similar rates of externalization for both peptides.

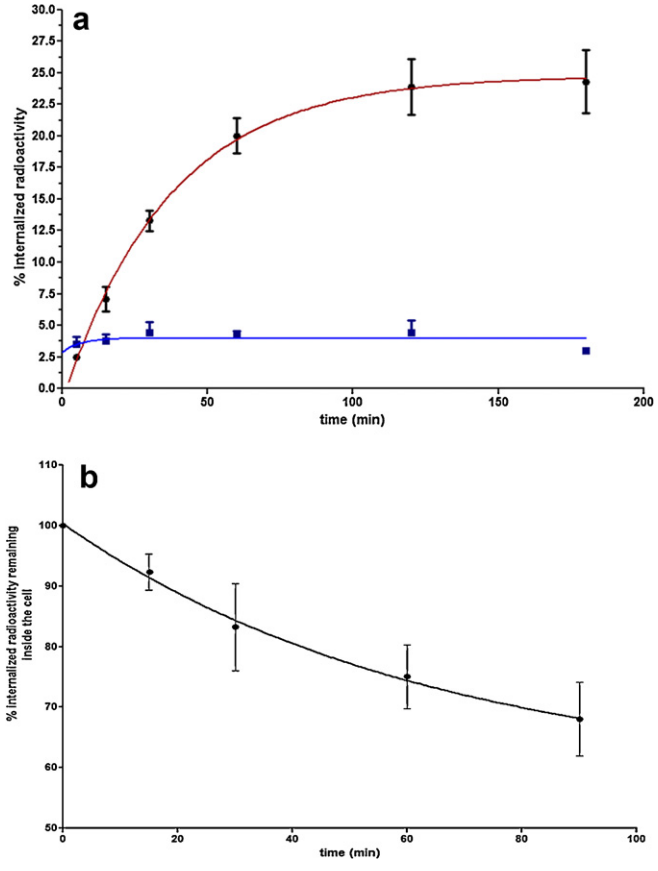

Fig. 6. Time course internalization of **^{99m}Tc-BN-A** in PC-3 cells at 37 °C presented as the % percentage of the total added radioactivity that was internalized into the cells (a); specific internalization (●), nonspecific internalization in the presence of native BN (■). Efflux determination of **^{99m}Tc-BN-A** (b) in PC-3 cells at 37 °C presented as the % percentage of the radioactivity that remained inside the cells after 2 h (time = 0 min) of initial incubation (●) against time.

3.7. Biodistribution analysis

3.7.1. Normal Swiss mice

Comparative in vivo studies in normal mice at 5, 15, 30, 60, 90, 120 min p.i. for both derivatives studied are reported in Fig. 7. Both ^{99m}Tc-BN species showed fast blood clearance. Although **^{99m}Tc-BN-A** presented higher blood values than **^{99m}Tc-BN-O** (9.47 ± 1.12 compared to 4.92 ± 0.65% ID/g respectively) 5 min p.i., blood concentration rapidly decreased 15 min p.i. at values lower than the ones of **^{99m}Tc-BN-O**, indicating a faster blood clearance. Heart values displayed a similar kinetic pattern for both peptides, with **^{99m}Tc-BN-A** presenting a higher value at 5 min p.i., which was rapidly decreased thereafter. A similar behaviour was observed in the lungs, where the uptake (8.91 ± 0.87% ID/g) for **^{99m}Tc-BN-A** was rapidly decreased, below 5%, at 15 min p.i., while for **^{99m}Tc-BN-O** it remained below 5% during the whole experiment. For both peptides, the values of % ID per gram for the above organs seemed closely related to the corresponding values in blood, thus indicating a correlation between the kinetic pattern of the peptide biodistribution in those specific organs and blood clearance. Muscle and spleen uptake for both peptides were insignificant and showed a similar pattern. In addition, insignificant uptake was also observed in the stomach, indicating that there is minimal, if any, leakage of free $^{99m}TcO_4^-$ due to the in vivo removal of ^{99m}Tc from the Gly-Gly-Cys- chelating group. Liver uptake was higher for **^{99m}Tc-BN-A**, 5 min p.i. (9.90 ± 1.31% ID/g), but it was decreased below 5% at 30 min p.i. Liver values for all the studied time-points for **^{99m}Tc-BN-O** remained relatively low (<5% ID/g). Intestinal uptake was also relatively low. The predominant excretion route for both BN derivatives studied was via the kidneys to the urine. The high kidney retention observed could be attributed to the increase in their overall charge, due to the presence of positively charged amino acids in their spacer chain. For **^{99m}Tc-BN-A,** urine values reached 63.34%ID/organ at 60 min p.i., while a similar value (63.15% ID/organ) was observed for **^{99m}Tc-BN-O** at 120 min p.i. The **^{99m}Tc-BN-O** urine value at 60 min p.i. was 30.58% ID/organ. In agreement with the above **^{99m}Tc-BN-A** displayed high kidney uptake for the first 30 min p.i., which was rapidly decreased thereafter. For **^{99m}Tc-BN-O** there was a time delay in the kidney uptake. The kidney values observed after 30 min p.i. were all higher than the respective ones for **^{99m}Tc-BN-A**, while the kidney clearance for **^{99m}Tc-BN-O** was slower. Finally, **^{99m}Tc-BN-A** presented high uptake in the pancreas, a GRPr-positive tissue, with an initial value of 14.07 ± 2.18% ID/g and values that remained above 9.0% ID/g until 120 min p.i. Both peptides reached their pancreas accumulation peak 15 min p.i., which was about 24.0 (% ID/g).

3.7.2. PC-3 tumor-bearing SCID mice

The results of the in vivo analysis in PC-3 tumor-bearing mice are presented in Fig. 8 and Table 4. Tumor sizes in this study were between 0.2 and 0.5 g. The high blood values observed for **^{99m}Tc-BN-A** at 15 min p.i. (7.14 ± 1.4% ID/g) were rapidly decreased within 60 min (0.8 ± 0.16% ID/g). **^{99m}Tc-BN-A** was capable of rapidly targeting the GRPr positive PC-3 tumor at 15 min p.i. (6.94 ± 0.50% ID/g). **^{99m}Tc-BN-A** also targeted the GPRr rich pancreas, presenting values around 24% ID/g, 15–30 min p.i., which decreased thereafter. Blocking studies for **^{99m}Tc-BN–A**, performed by the co-administration of an excess amount of native BN 30 min p.i., decreased pancreas accumulation. In agreement with the biodistribution results of **^{99m}Tc-BN-A** in normal mice, the predominant excretion route for the PC-3 tumor-bearing SCID mice was via the kidney to the urine.

For **^{99m}Tc-BN-A**, as can be observed in Fig. 8, the tumor/blood contrast ratio increased until 120 min, when it reached its highest value (4.53). The tumor/muscle ratio, which was high already at 15 min p.i. (4.74), reached its peak at 30 min p.i. (8.86),

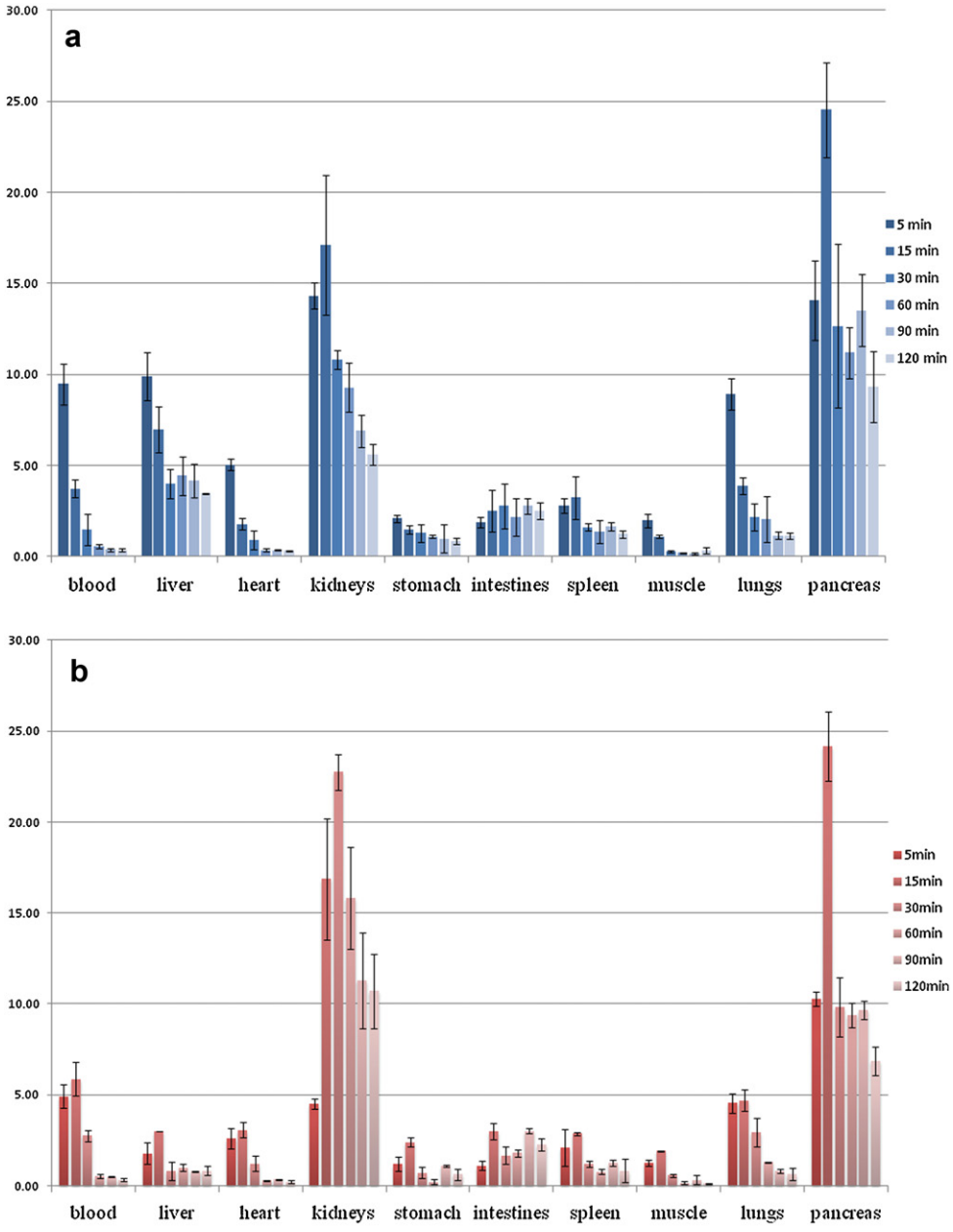

Fig. 7. Biodistribution results in normal female mice expressed as % ID/g for ^{99m}**Tc-BN-A** (a) and ^{99m}**Tc-BN-O** (b).

decreased at 60 min (5.60) and increased again at 120 min (8.65). The tumor/intestines ratio presented its highest value at 15 min p.i. (2.0), gradually decreasing until 120 min p.i. (1.25). The tumor/kidneys and tumor/liver ratios presented similar and rather stable values which were also decreased 120 min p.i. The low values observed for ^{99m}**Tc-BN-A** considering the tumor/kidneys contrast ratio were expected since it was designed to be excreted through the urinary pathway.

Comparing these results with the ones previously reported for the BN analogue with the ornithine spacer (Fragogeorgi et al., 2009) we observe that for ^{99m}**Tc-BN-O** there was also a high load of radioactivity in the bladder and the kidneys, while additionally the tumor and the total animal radioactivity decrease at a slower rate. ^{99m}**Tc-BN-O** presented comparable tumor/blood contrast values (1.57) with ^{99m}**Tc-BN**-A at 30 min p.i. (1.86), which increased afterwards (33.32 at 120 min p.i.). The tumor/kidneys contrast ratio was higher for ^{99m}**Tc-BN-A** at 60 min p.i. and lower at 30 and 120 min (0.39, 0.27 and 0.28 respectively) than the respective ones of ^{99m}**Tc-BN-O** (0.28, 0.52 and 0.48). The tumor/muscle ratio was higher for ^{99m}**Tc-BN-A** until 30 min p.i. (8.86 against 6.38) and decreased to values lower than those of ^{99m}**Tc-BN-O** thereafter. Tumor/liver ^{99m}**Tc-BN-A** contrast values were at all time-points lower than the ones of ^{99m}**Tc-BN-O**. Tumor/intestines ^{99m}**Tc-BN-A** values were marginally higher (1.25) than the respective ones of ^{99m}**Tc-BN-O** at 120 min p.i. (1.17), while for all other time points they were lower. Although for the intestines, factors like food uptake should also be taken into account.

3.8. Pharmacokinetic analysis

Blood values (% ID/g) for both peptides were plotted against time applying pharmacokinetic (PK) compartment models (Fig. 9). The F-test and the Akaike Information Criteria (AIC) were used for the choice of the best model (Table I of supplementary material).

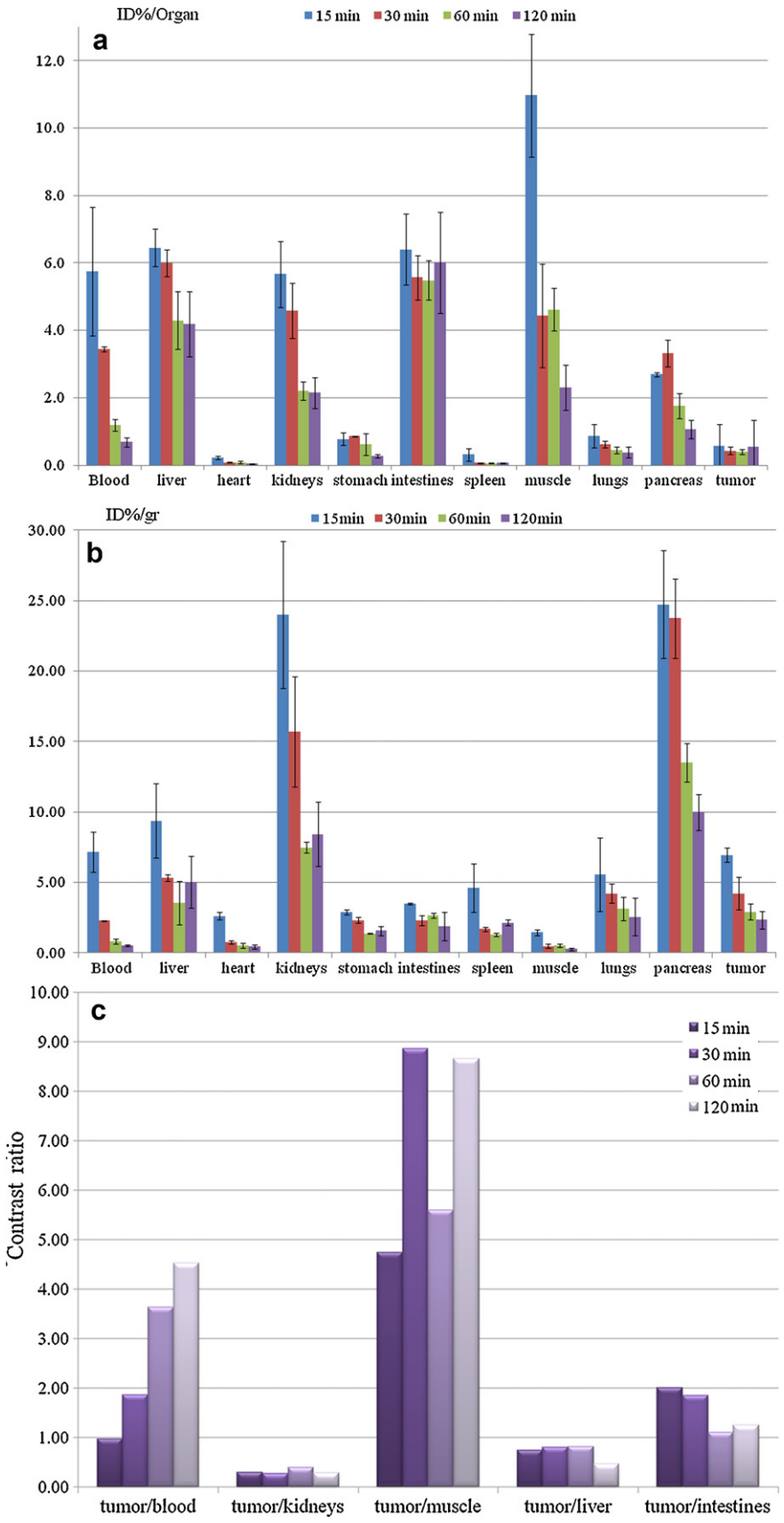

Fig. 8. Biodistribution results for ^{99m}**Tc-BN-A** in PC-3 tumor-bearing SCID female mice expressed as %ID/organ (a), %ID/g (b); Contrast ratios for ^{99m}**Tc-BN-A** in PC-3 tumor-bearing, female SCID mice (c).

Table 3
PK data for **^{99m}Tc-BN-A** and **^{99m}Tc-BN-O**.

^{99m}Tc-BN–A

Best fit model	A	a	B	b	$t_{1/2a}$ (min)	$t_{1/2b}$ (min)
$C = A \times e^{(a \times t)} + B \times e^{(b \times t)}$	14.4 (1.59)[a]	−0.103 (0.012)[a]	0.827 (0.245)[a]	−0.008 (0.003)[a]	6.73[a]	86.64[a]

	C_{max}[b] (%ID/g)	t_{max} (min)	AUC (%ID × min/g)	AUMC (%ID × min^2/g)	MRT (min)
Blood	–	5	220.7[c]	4727	21.42
Liver	9.90 (1.31)	5	560.3	29753	53.10
Heart	5.03 (0.32)	5	105.7	3278	31.01
Kidneys	17.12 (3.85)	15	1134	56458	49.79
Stomach	2.09 (0.19)	5	122.2	7141	58.44
Intestines	2.77 (0.44)	90	292.8	18257	62.35
Spleen	3.23 (1.19)	15	206.1	10914	52.95
Muscle	1.96 (0.37)	5	50.13	1848	36.86
Lungs	8.91 (0.87)	5	276.5	11328	40.97
Pancreas	24.54 (2.61)	15	1578	87078	55.18

^{99m}Tc-BN–O

Best fit model	A	a	B	b	$t_{1/2a}$ (min)	$t_{1/2b}$ (min)
$C = A \times e^{(a \times t)}$	5.9 (1.5)[a]	−0.030 (0.005)[a]	–	–	23.5[a]	–

	C_{max}[b] (% ID/g)	t_{max} (min)	AUC (%ID × min/g)	AUMC (%ID × min^2/g)	MRT (min)
Blood	–	15	223.1[c]	6048	27.11
Liver	2.98 (0.010)	15	117.4	5013	42.70
Heart	3.08 (0.42)	15	107.7	3335	30.97
Kidneys	22.75 (0.97)	30	1730	96917	56.02
Stomach	2.40 (0.24)	15	103.7	5447	52.53
Intestines	2.99 (0.45)	15	262.2	17246	65.77
Spleen	2.86 (0.07)	15	152.0	7713	50.74
Muscle	1.91 (0.03)	15	62.43	2159	34.58
Lungs	4.70 (0.58)	15	232.8	8794	37.77
Pancreas	24.17 (1.89)	15	1275	66923	52.49

[a] Values calculated after the fitting of the appropriate model.
[b] Experimental values expressed as a mean of 3–4 animals with the SD in the parenthesis.
[c] For the calculation of blood AUC by the trapezoid rule for $t = 0$ min we used the values calculated for concentration after the model fitting $C^0_{BN\text{-}A} = 14.4\%$ ID/g; $C^0_{BN\text{-}O} = 5.9\%$ ID/g.

^{99m}Tc-BN-A followed a two compartment model, while for **^{99m}Tc-BN-O** the one compartment model proved a better fit. From the %ID/g–time plots the Area Under the Curve (AUC) values were calculated for each organ until 120 min, using the trapezoid rule and the results are summarized in Table 3. For the initial ($t = 0$ min) blood values, the ones calculated from the best fitting PK model were used, while for the other organs the initial values were considered to be % ID/g = 0 ($t = 0$ min). The AUC, which derives from drug concentration and time, can be used as a measure of drug exposure. In other words it gives a measure of how much and of how long a drug stays into the specific organ of the body. The GRPr rich pancreas and the kidneys presented the highest AUC values for both peptides, while muscles the lowest one. Liver AUC was high for **^{99m}Tc-BN-A**, with values being about 80% higher than the respective ones for **^{99m}Tc-BN-O**, a fact which indicated a higher and longer liver accumulation of this derivative. Kidney AUC values also showed differences between the two BN analogues, with the value for **^{99m}Tc-BN-O** (1730% ID × min/g) being 53% higher than the one for **^{99m}Tc-BN-A** (1134% ID × min/g). Although both peptides presented high kidney accumulation, the **^{99m}Tc-BN-A** seemed to clear faster. **^{99m}Tc-BN–A** presented lower AUC_{blood} (220.7% ID × min/g) and greater clearance (CL = 0.453% ID/g/min) values than **^{99m}Tc-BN–O** (AUC_{blood} = 223.1% ID × min/g, CL = 0.448% ID/g/min).

3.9. Imaging studies

Tumor localization of **^{99m}Tc-BN-A** in PC-3 tumor-bearing mice exhibited a considerable tumor uptake as shown by γ-ray scintigraphy. The PC-3 tumor at the right front flank was visible with clear contrast from the adjacent background, as early as 10 min p.i. and remained observable up to 60 min p.i. Prominent uptake was also observed in the kidneys, while the clearance of the radioactivity through the urinary bladder was also evident (Fig. 10). An imaging analysis was performed where two Regions Of Interest (ROIs) were chosen: one around the visible tumor area and one containing normal tissue, for those ROIs the % ID were calculated as a ratio of the counts of each ROI against the total counts and plotted against time (Fig. 10). The results of the above imaging analysis were in agreement with the ones obtained from the biodistribution of PC-3 tumor-bearing mice. The images from the analysis of **^{99m}Tc-BN-A** and **^{99m}Tc-BN-O** were combined into animated video (Video 1) and (Video 2) respectively.

4. Discussion

Various factors may influence tumor uptake and body retention of radiolabelled peptides, such as: their binding affinity for the receptors, expressed on the surface of the tumor, the population of these receptors and the in vivo stability, as well as the pharmacokinetic profile of the radiotracers themselves (Nanda et al., 2010). Different approaches have recently been followed concerning the improvement of the tumor-targeting ability of radiolabelled BN analogues by using different types of peptide sequences, metal chelators and spacer groups (Okarvi, 2004; Smith et al., 2005)

The present study is focused on the effect of incorporating a positively charged aa spacer group and a N_3S-type aa chelator group (Gly-Gly-Cys-) to the pharmacophore group BN(2–14) for the utilization of BN-like peptides as radiodiagnostics. In other words, two BN-like peptides (**M-BN-A**, **M-BN-O**; M = ^{99m}Tc or $^{185/187}$Re) with a positively charged aa spacer chain were comparatively evaluated

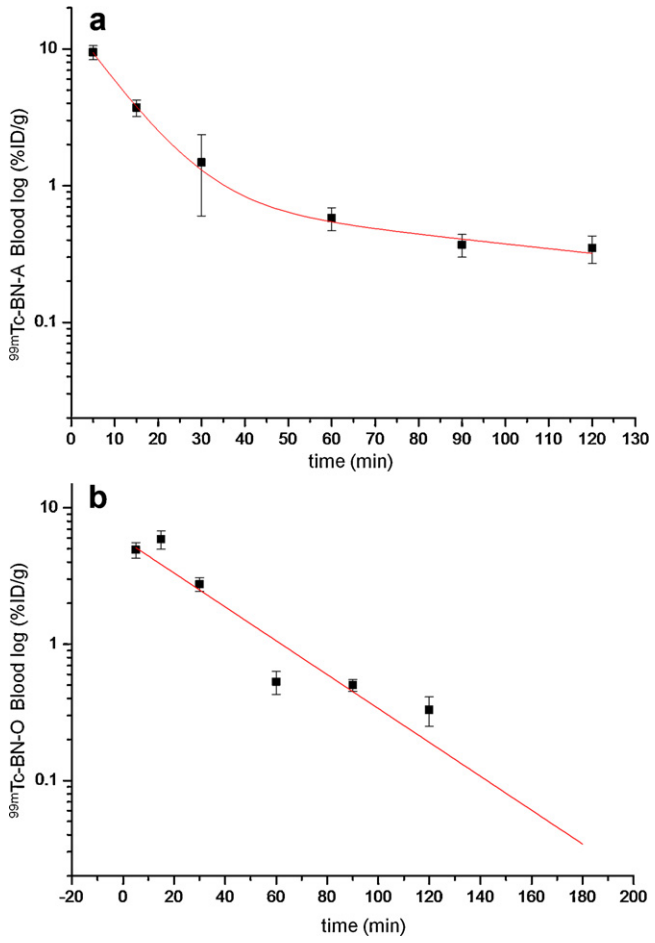

Fig. 9. The curves that best fitted the blood log(% ID/g) vs time values according to the compartmental analysis of **^{99m}Tc-BN-A** (a), two compartment; and of **^{99m}Tc-BN-O** (b), one compartment.

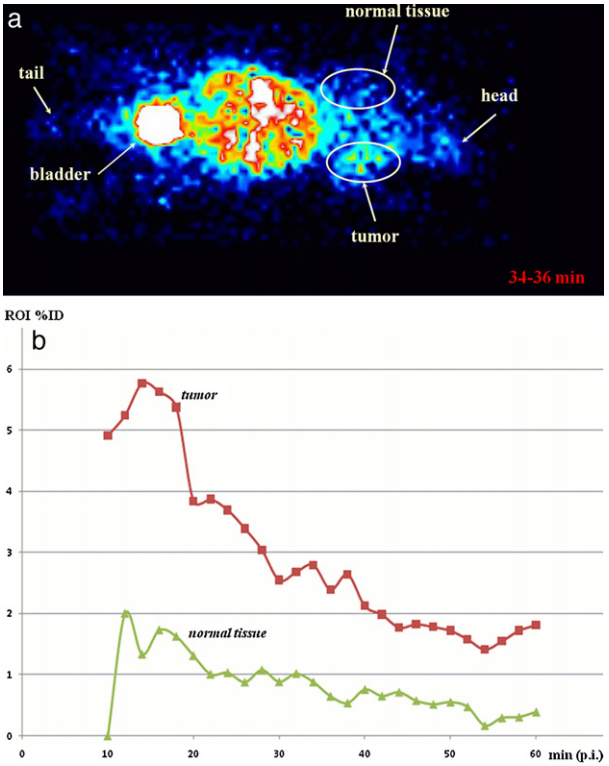

Fig. 10. A typical, 2 min frame (34–36 min), scintigraphic image of a tumor-bearing mouse for **^{99m}Tc-BN-A**, where the tumor and the normal tissue ROIs are indicated by circles (a). Graph representing the ROIs' analysis of the tumor (■) in comparison with the normal tissue (▲) (b).

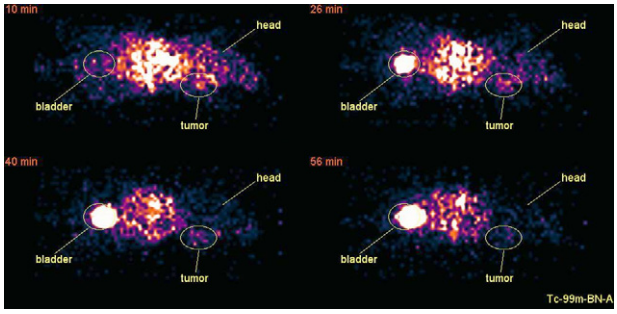

Video 1. Static images at selected time points from scintigraphic dynamic imaging video analysis of a tumor- bearing mouse for **^{99m}Tc-BN-A**.

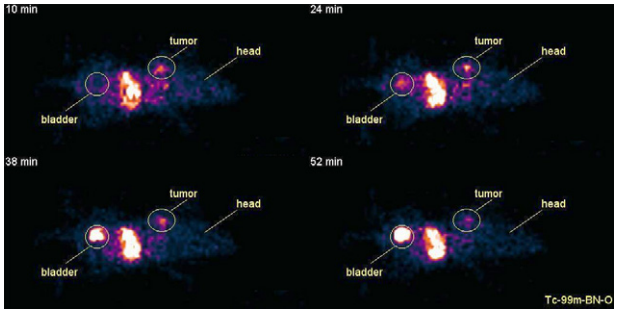

Video 2. Static images from Gamma-ray dynamic imaging video analysis of a tumor-bearing mouse for **^{99m}Tc-BN-O**.

in vitro for their labelling efficiency, their plasma stability, their binding affinity to GRPrs, their internalization/externalization rates in PC-3 cells and in vivo for their biodistribution profile, pharmacokinetic characteristics and tumor-targeting ability. The results of the above study are being compared with the ones of similar BN-like peptides referred in the literature and, whenever possible, results concerning structural modifications and favorable characteristics are being drawn.

The peptide chelate sequence Gly-Gly-Cys- forms stable neutral N_3S complexes with the metal, M (M = ^{99m}Tc, $^{185/187}$Re), where the $M^{(V)}$oxo core coordinates via the mercapto atom (-Cys-), the two amide nitrogen atoms (-Gly-Cys-) and the N-terminal amine nitrogen atom (Gly-) (Lister-James et al., 1996; Jankowsky et al., 1998; Gourni et al., 2009). Both spacer chains used: -(arginine)$_3$- and -(ornithine)$_3$-, consist of positively charged amino acids. The 3-carbon side chain of arginine (**BN-A**) is capped by a complex guanidinium group $[CH_6N_3]^+$, while the 3-carbon side chain of ornithine (**BN-O**) is capped with an amino group $[NH_3]^+$. The guanidinium group has a pK_a of 12.48 and is positively charged in neutral, acidic and even most basic environments. The $[NH_3]^+$ group, with a pK_a of 10.76, is also positively charged, although it can be considered as a slightly weaker base than the former. The BN(2–14) peptide chain has been chosen since BN analogues, which maintain their amidated C-terminal methionine intact, have been shown to be agonists (Mantey et al., 1993). In contrast to radiolabelled antagonists, radiolabelled BN agonists are internalized into GRPr-positive cells (Breeman et al., 1999a,b) presenting thus a wide potential for tumor imaging, since their internalization results in a higher accumulation of radioactivity into GRPr positive tissues, provided that cell washout of the internalized radioactive species does not occur (Van de Wiele et al., 2001a).

In the present study both complexes of **BN-A** and **BN-O** with ^{99m}Tc were easily formed in high yield (>98%). The claim that $^{185/187}$Re-BN and ^{99m}Tc-BN derivatives have the same structure was also verified by their similar Rt after co-injection on a RP-HPLC column (Fig. 2). The above results were consistent with previous studies, which demonstrated that N_3S type ligand systems such as Gly-Gly-Cys- form stable ^{99m}Tc-peptide conjugates, in high yield and specific activity after the transchelation of $^{185/187}Re^{(V)}/^{99m}Tc^{(V)}$ from the gluconate precursors (Wong et al., 1997; Alves et al., 2006; Fragogeorgi et al., 2009; Gourni et al., 2009). The addition of the positively charged spacer chain did not seem to affect the labelling efficiency of the Gly-Gly-Cys- chelator, while the Rt difference between the two labelled products could be attributed to the additional MW of the -(arginine)$_3$- spacer.

The stability of both BN derivatives was determined in vitro, in mouse and human plasma. Over 60% of both tested radiolabelled BN derivatives remained intact after 1 h incubation in human plasma, while peptide metabolism was much faster in mouse plasma. Such differences between species should be considered during preclinical studies, when mediocre results are observed for mice before discarding possible candidates for further studies. This observation is also in agreement with similar studies in the literature on BN analogues, conducted in different species (Linder et al., 2009; Gu et al., 2011), where the in vitro plasma metabolites were found to be the same across species (mouse, rat and human plasma), but their relative amounts were diverce. These differences are assumed to be due to the different metabolic rates and enzymes between the species. The appearance of a major radioactive metabolite, with Rt close to that of the intact peptide, could probably be related to a metabolic process, in which the amino acids of the C terminus are more susceptible. Previous studies on BN derivatives have shown that cleavage could occur between His^{12}-Leu^{13} (Shipp et al., 1991; Linder et al., 2009), although further proof is needed. The slight resistance of **^{99m}Tc-BN-O** compared with **^{99m}Tc-BN-A**, to the catabolic action of peptidases in the plasma could be attributed to the fact that the latter contained the natural aa arginine in its spacer chain, which is more susceptible than ornithine to their actions.

The affinity of the radiolabelled BN derivates for the GRPrs is crucial for their efficiency as potential radiodiagnostic or radiotherapeutic agents. The binding affinity of **BN-A**, **BN-O** and their $^{185/187}$Re complexes for the GRPr were similar and compared to the one of the standard [Tyr^4]-BN (Table 2). According to the results of the internalization studies (Fig. 6), **^{99m}Tc-BN-A** seems to be a weaker agonist than **^{99m}Tc-BN-O**, since it needs more time to reach its maximum amount of internalization (plateau). Parry et al., 2007, have reported the hypothesis that the incorporation of a negatively charged glutamic acid spacer decreases the binding affinity of the BN(7–14) for the GRPr. In the present study, it has been demonstrated that a positively charged amino acid spacer, composed either from arginine or ornithine, did not decrease the binding affinity of BN(2–14), although there was a reduction of its agonistic ability, when the spacer was composed of arginine. Presumably this could be related to the pK_a value (12.48) and to the structure of the positively charged guanidine group, capping the 3-carbon side chain of arginine. Consequently, the binding affinity, as well as the agonistic ability of a BN analogue could be affected by: (i) the type of the charge (positive/negative, pK_a) and (ii) the total net charge value of the amino acid spacer. The latter should probably be viewed in coalition with the total net charge value of the rest of the peptide chain and the chelator–metal complex.

Additionally to a high affinity for the target receptor the ideal radiodiagnostic product characteristics should also include a high tumor uptake combined with rapid clearance from blood and non-target tissues. The preferred route of excretion in most cases is the renal system since in this way the upper abdominal radioactivity is reduced (Van de Wiele et al., 2001a; Okarvi, 2004; Lee et al., 2010).

Table 4
Biodistribution of **^{99m}Tc-BN-A** in PC-3 tumor-bearing SCID female mice.

% ID per organ	15 min	30 min	60 min	120 min
Blood	5.75 ± 1.91	3.45 ± 0.07	1.19 ± 0.18	0.69 ± 0.13
Liver	6.45 ± 0.56	6.00 ± 0.40	4.30 ± 0.86	4.19 ± 0.95
Heart	0.22 ± 0.04	0.08 ± 0.01	0.09 ± 0.04	0.04 ± 0.02
Kidneys	5.67 ± 0.98	4.59 ± 0.82	2.21 ± 0.28	2.15 ± 0.46
Blocked kidneys	ND	7.76 ± 1.50	ND	ND
Stomach	0.78 ± 0.17	0.87 ± 0.01	0.63 ± 0.32	0.27 ± 0.05
Intestines	6.40 ± 1.06	5.57 ± 0.65	5.49 ± 0.58	6.02 ± 1.50
Spleen	0.32 ± 0.19	0.07 ± 0.01	0.06 ± 0.02	0.07 ± 0.02
Muscle	10.97 ± 1.82	4.45 ± 1.54	4.62 ± 0.64	2.30 ± 0.67
Lungs	0.87 ± 0.34	0.63 ± 0.10	0.45 ± 0.10	0.38 ± 0.17
Pancreas	2.69 ± 0.07	3.32 ± 0.40	1.77 ± 0.37	1.07 ± 0.27
Blocked pancreas	ND	0.46 ± 0.01	ND	ND
Tumor	0.56 ± 0.66	0.43 ± 0.10	0.41 ± 0.08	0.55 ± 0.80
Blocked tumor	ND	0.20 ± 0.13	ND	ND
Urine*	1.03	32.30	33.97	29.42
% ID per gram	**15 min**	**30 min**	**60 min**	**120 min**
Blood	7.14 ± 1.42	2.27 ± 0.05	0.80 ± 0.16	0.52 ± 0.07
Liver	9.38 ± 2.62	5.31 ± 0.22	3.55 ± 1.55	5.03 ± 1.85
Heart	2.61 ± 0.28	0.74 ± 0.11	0.50 ± 0.17	0.43 ± 0.14
Kidneys	24.01 ± 5.21	15.69 ± 3.91	7.48 ± 0.40	8.42 ± 2.29
Blocked kindeys	ND	33.73 ± 4.45	ND	ND
Stomach	2.87 ± 0.18	2.32 ± 0.19	1.37 ± 0.01	1.58 ± 0.33
Intestines	3.47 ± 0.05	2.29 ± 0.37	2.65 ± 0.17	1.88 ± 1.00
Spleen	4.60 ± 1.72	1.70 ± 0.15	1.31 ± 0.12	2.14 ± 0.23
Muscle	1.46 ± 0.21	0.48 ± 0.16	0.52 ± 0.13	0.27 ± 0.10
Lungs	5.55 ± 2.63	4.20 ± 0.68	3.14 ± 0.82	2.56 ± 1.32
Pancreas	24.73 ± 3.81	23.75 ± 2.83	13.51 ± 1.38	9.99 ± 1.27
Blocked pancreas	ND	5.13 ± 1.0	ND	ND
Tumor	6.94 ± 0.50	4.22 ± 1.17	2.90 ± 0.57	2.35 ± 0.62
Blocked tumor	ND	1.1 ± 0.25	ND	ND

ND: not defined.
* The maximum values observed for urine are reported.

In the present study both BN peptides studied displayed a high uptake in the tumor, combined with rapid blood clearance, while the main route of excretion was the renal system. High uptake in non target GRPr positive tissues such as the pancreas in relation to the targeted tumor uptake could be considered a limiting factor for peptide targeted tumor therapy. The high pancreatic uptake was to be expected for radiolabelled BN analogues since pancreas is an organ with high GRPr expression. Previous reports have suggested co- or pre- injection of excess amounts of cold BN agonists or preferably antagonists, in order to reduce pancreatic uptake of the radiolabelled BN analogue (Lantry et al., 2006; de Visser et al., 2007, 2008). In this study (Table 4) as well as in previous studies of our laboratory (Gourni et al., 2009) we have also observed a higher reduction in the pancreatic than in the tumoral radioactivity uptake, when cold BN was pre-injected.

One of the major factors affecting kidney accumulation and retention is the overall charge of the radiometal–chelator–spacer conjugate and its effect on the hydrophilicity of the molecule, especially referring to peptides with similar spacer moieties (Rogers et al., 2003; Biddlecombe et al., 2007; Parry et al., 2007). One of the processes that can influence the residence time of radiolabelled peptides into the kidneys is tubular reabsorption (Akizawa et al., 2008). This can be manipulated by making use of the electrostatic interaction between the negatively charged surface of the proximal tubular cells and the cationic portion of peptides e.g. renal accumulation of radiolabelled peptides can be reduced by lysine treatment (de Jong et al., 1996; Bernard et al., 1997; Rolleman et al., 2003; Gotthardt et al., 2007). According to the literature, the re-absorption of the peptides may be due to an interaction between the negatively charged megalin receptor, at the proximal tubule cell surface and the positively charged peptide. The receptor-mediated endocytosis and peptide reabsorption could be prevented by blocking the receptor with an external administration of

positively charged amino acids (Gotthardt et al., 2007; de Jong et al., 2005). However, the large amounts of charged amino acids needed (hyperosmolar solutions) to achieve the reduction of peptide renal uptake, often result in side effects, such as hyperkalemia, vomiting, volume overload, and local irritation at the injection site (Rolleman et al., 2003). Thus, we decided to try the incorporation of positively charged amino acids in the peptide backbone as a spacer chain. Additionally in the case of the more polar arginine our goal was the achievement of faster blood and kidney clearance which would also result in decreased kidney radioactivity exposure as well as the optimum tumor/background ratios. Confirming our hypothesis both BN peptides studied displayed a high kidney uptake in normal mice (Fig. 7), which decreased at different rates. **^{99m}Tc-BN-A** was cleared faster from the blood and the body than **^{99m}Tc-BN-O**, indicative of an improvement in its body clearance rate and its kidney retention time. The PK time delay observed for **^{99m}Tc-BN-O**, probably could be attributed to the small difference in the structure and pK_a values between their side chains, as previously mentioned.

Blood concentration values for **^{99m}Tc-BN-A** and **^{99m}Tc-BN-O** followed a second ($t_{1/2a}$ = 6.73 min, $t_{1/2b}$ = 86.64 min) and a first order elimination ($t_{1/2a}$ = 23.5 min) model respectively. The highest AUC and AUMC value of **^{99m}Tc-BN-A** and of **^{99m}Tc-BN-O** were for the pancreas and for the kidneys, with **^{99m}Tc-BN-A** presenting its top values for the pancreas and **^{99m}Tc-BN-O** for the kidneys (Table 3). The high AUC, AUMC liver values of **^{99m}Tc-BN-A** in comparison with the ones of **^{99m}Tc-BN-O** could probably be attributed to the susceptibility of **^{99m}Tc-BN-A** to liver enzymes or to the presence of a radioactive metabolite, which follows the hepatobiliary excretion path. This is also supported by the fact that **^{99m}Tc-BN-A** and **^{99m}Tc-BN-O** presented major differences in liver and kidney MRT values, while MRT for the blood and the rest of the organs examined were similar. The latter is also indicative of similarities in PK pattern for those organs.

A direct comparison of **^{99m}Tc-BN-A** and **^{99m}Tc-BN-O** with other ^{99m}Tc-labelled bombesin derivatives concerning the influence of the spacer group in the biodistribution, the PK profile and the tumor uptake, is rather difficult, since in most of the reports, the C-terminally amidated BN(7–14) sequence or other stabilized forms were studied and different chelator groups were used. The long BN(2–14) peptide chain contains an additional positively charged arginine aa residue and the different chelators apart from the total peptide charge might also influence the peptide receptor affinity. Despite this, in some cases a number of conclusions could be drawn for similar BN derivatives.

Data from the PK analysis of radiolabelled BN analogues are scarce in recent literature. Rogers et al. (1997) have performed a PK analysis for [^{125}I-Tyr^4]-BN and [^{125}I]-mIP-Des-Met^{14}-BN(7–13), in normal mice. [^{125}I]-mIP-Des-Met^{14}-BN(7–13) better fitted a two compartment model by showing an early rapid distribution ($t_{1/2a}$ = 6 min) and a slower elimination phase ($t_{1/2b}$ = 8 h), whereas [^{125}I-Tyr^4]-BN cleared from blood and other tissues with a first order elimination rate ($t_{1/2a}$ = 132 min). A similarity concerning the distribution phase of [^{125}I]-mIP-Des-Met^{14}-BN(7–13) and **^{99m}Tc-BN-A** (~6 min) can be observed, although the major structural differences between those compounds and the peptides in this study make a possible structural–PK correlation rather difficult.

In previous studies of our group on ^{99m}Tc-labelled BN derivatives the long BN(2–14) sequence was either directly attached to the N_3S chelator (Fragogeorgi et al., 2009) (**BN-N**, MW = 1725.8) or through a 6-aminohexanoic acid spacer (**BN-Aca**, MW = 1839.14) (Gourni et al., 2009). In both cases there was no addition of charges in the total peptide charge. If the no-spacer sequence is considered as the essential part for an effective ^{99m}Tc-labelled BN derivative, the 6-aminohexanoic acid spacer added 6.57% in the MW of this basic structure (**BN-Aca**), -(arginine)$_3$-, 27.19% (**BN-A**) and -(ornithine)$_3$-, 19.85% (**BN-O**).

In reference to the receptor rich pancreas, the radiolabelled peptide **^{99m}Tc-BN-N**, which was closer to the basic BN structure and the **^{99m}Tc-BN-Aca**, both presented similar values in normal mice 30 and 60 min p.i. (Fragogeorgi et al., 2009; Gourni et al., 2009). Pancreatic values in normal mice for the positively charged **^{99m}Tc-BN-A** and **^{99m}Tc-BN-O** were also at similar levels with the previously referred peptides at 30 min p.i., while they remained significantly higher even 60 min p.i. The main route of excretion for the positively charged spacer chain peptides was the urinary system, thus their kidney values were significantly higher than the ones of **^{99m}Tc-BN-N** and **^{99m}Tc-BN-Aca**. For **^{99m}Tc-BN-A** the highest kidney value (24.01 ± 5.21%ID/g) was observed at 15 min p.i. and it decreased afterwards, while for **^{99m}Tc-BN-O** the highest value was observed at 60 min p.i. and decreased thereafter. Thus, despite the MW increase, the addition of charged amino acid spacers in the BN basic structure had the desirable effect on the PK characteristic concerning their excretion route.

Considering the PC-3 tumor-bearing mice, the tumor accumulation peak was observed for **^{99m}Tc-BN-A** was between 15 and 30 min p.i. (6.94 ± 0.50; 3.40± 1.17%ID/g), while for **^{99m}Tc-BN-O** between 60 and 120 min p.i. (7.14 ± 0.87; 7.92 ± 0.79%ID/g). For **^{99m}Tc-BN-N** and **^{99m}Tc-BN-Aca** the tumor accumulation peak was observed at 30 min p.i. (4.56 ± 0.95 and 4.9 ± 0.5% ID/g respectively, the differences between **^{99m}Tc-BN-N** and **^{99m}Tc-BN-Aca** being not statistically significant as determined by the *t*-test).

Although additional data are needed for a safe conclusion to be drawn, it seems that the addition of a charged 3 carbon long spacer led to derivatives superior than the ones without spacer or the ones with a neutral 3 carbon spacer, since it led to higher tumor uptake with the additional advantages of fast blood clearance and renal excretion. Concerning the differences between the two BN-like peptides with the positively charged spacer chains, **^{99m}Tc-BN-A** presented a faster clearance from the tumor than **^{99m}Tc-BN-O**, which was probably due to its faster clearance from the body in general. In conclusion, **^{99m}Tc-BN-A** was cleared faster from the body, as well as from the tumor and presented lower kidney accumulation and faster kidney clearance; **^{99m}Tc-BN-O** while maintaining a high tumor uptake for a longer time period, presented a higher kidney accumulation.

The results of the present study, which examined thoroughly the effect of the spacer chain in-between the pharmacophore peptide and the radionuclide chelator site, may be extended to other peptides targeting the G-protein coupled receptors.

5. Conclusions

The structural changes introduced in the N_3S-BN(2–14) derivatives, via the addition of a charged aa spacer chain proved promising for the visualization of GRP receptors, expressed at cell membranes of various cancer tissues. Both derivatives studied in the present work resulted in ^{99m}Tc-labelled BN species with high affinity for GRPrs and optimal PK profile. In general as shown in this and previous studies of our group, tumor accumulation and contrast ratio (tumor/normal tissues) seems to be affected by a variety of factors such as: the total peptide charge, the length of the peptide sequence, the MW and the presence of non-natural amino acids, which also influence the affinity, the biodistribution, and the PK profile of the ^{99m}Tc-labelled BN like peptides. A detailed evaluation of those factors would likely result in the optimal characteristics, which a BN derivative should avail, in order to render effective its clinical application, as an imaging or therapeutic agent. If the tumor is considered as another PK compartment, it becomes clear that tumor accumulation would be strongly influenced by the rate of blood and body clearance of the BN peptide, apart from its affinity for the GPRrs. Additional data are needed in order to find a way

to further reduce non target organ (i.e. kidney, pancreas) exposure without reducing tumor uptake for analogues like **^{99m}Tc-BN-A** and **^{99m}Tc-BN-O**. Research in designing novel radiolabelled BN-like peptides should be further directed towards the determination of possible correlations, between the structural and the pharmacokinetic and pharmacodynamic characteristics.

Appendix A. Supplementary data

Supplementary data associated with this article can be found, in the online version, at doi:10.1016/j.ijpharm.2012.02.049.

References

Akizawa, H., Uehara, T., Arano, Y., 2008. Renal uptake and metabolism of radiopharmaceuticals derived from peptides and proteins. Adv. Drug Deliv. Rev. 60 (12), 1319–1328.

Alves, S., Paulo, A., Correia, J.D., Santos, I., Gano, L., Veerendra, B.C.J., Sieckman, G.L., Hoffman, T.J., Rold, T.L., Figueroa, S.D., Retzloff, L., McGrate, J., Prasanphanich, A., Smith, C.J., 2006. Pyrazolyl conjugates of bombesin: a new tridentate ligand framework for the stabilization of fac-[M(CO)$_3$]+ moiety. Nucl. Med. Biol. 33, 625–634.

Ananias, H.I.K., De Jong, I.J., Dierckx, R.A., Van de Wiele, C., Helfrich, W., Elsinga, P.H., 2008. Nuclear imaging of prostate cancer with gastrin-releasing-peptide-receptor targeted radiopharmaceuticals. Curr. Pharm. Des. 14, 3033–3047.

Anastasi, A., Erspamer, V., Bucci, M., 1971. Isolation and structure of bombesin and alytesin, 2 analogous active peptides from the skin of the European amphibians Bombina and Alytes. Experientia 27, 166–167.

Anastasi, A., Erspamer, V., Bucci, M., 1972. Isolation and amino acid sequences of alytesin and bombesin, two analogous active tetradecapeptides from the skin of European discoglossid frogs. Arch. Biochem. Biophys. 148, 443–446.

Baidoo, K.E., Lin, K.S., Zhan, Y., Finley, P., Scheffel, U., Wagner, H.N., 1998. Design, synthesis, and initial evaluation of high-affinity technetium bombesin analogues. Bioconjugate Chem. 9, 218–225.

Bernard, B.F., Krenning, E.P., Breeman, W.A., Rolleman, E.J., Bakker, W.H., Visser, T.J., Macke, H., de Jong, M., 1997. D-lysine reduction of indium-111 octreotide and yttrium-90 octreotide renal uptake. J. Nucl. Med. 38, 1929–1933.

Biddlecombe, G.B., Rogers, B.E., De Visser, M., Parry, J.J., De Jong, M., Erion, J.L., Lewis, J.S., 2007. Molecular imaging of gastrin-releasing peptide receptor-positive tumors in mice using ^{64}Cu- and ^{86}Y-DOTA-(Pro^1, Tyr ^{4})-bombesin(1–14). Bioconjugate Chem. 18 (3), 724–730.

Blok, D., Feitsma, H.I.J., Kooy, Y.M.C., Welling, M.M., Ossendorp, F., Vermeij, P., Drijfhout, J.W., 2004. New chelation strategy allows for quick and clean ^{99m}Tc-labelling of synthetic peptides. Nucl. Med. Biol. 31, 815–820.

Breeman, W.A.P., de Jong, M., Bernard, B.F., Kwekkeboom, D.J., Srinivasan, A., van der Pluum, M., Hofland, L.J., Visser, T.J., Krenning, E.P., 1999a. Pre- clinical evaluation of [^{111}In-DTPA, Pro1, Tyr4] bombesin, a new radioligand for bombesin-receptor scintigraphy. Int. J. Cancer 83, 657–663.

Breeman, W.A.P., Hofland, L.J., de Jong, M., Bernard, B.F., Srinivasan, A., Kwekkeboom, D.J., Visser, T.J., Krenning, E.P., 1999b. Evaluation of radiolabelled bombesin analogues for receptor-targeted scintigraphy and radio-therapy. Int. J. Cancer 81, 658–665.

Cantorias, M.V., Howell, R.C., Todaro, L., Cyr, J.E., Berndorff, D., Rogers, R.D., Francesconi, L.C., 2007. MO tripeptide diastereomers (M = $^{99/99m}$ Tc, Re): models to identify the structure of ^{99m}Tc peptide targeted radiopharmaceuticals. Inorg. Chem. 46 (18), 7326–7340.

Chen, X., Park, R., Hou, Y., Tohme, M., Shahinian, A.H., Bading, J.R., Conti, P.S., 2004. microPET and autoradiographic imaging of GRP receptor expression with ^{64}Cu-DOTA-[Lys^3]bombesin in human prostate adenocarcinoma xenografts. J. Nucl. Med. 45 (8), 1390–1397.

de Jong, M., Barone, R., Krenning, E., Bernard, B., Melis, M., Visser, T., Gekle, M., Willnow, T.E., Walrand, S., Jamar, F., Pauwels, S., 2005. Megalin is essential for renal proximal tubule reabsorption of 111 In-DTPA-octreotide. J. Nucl. Med. 46, 1696–1700.

de Jong, M., Rolleman, E.J., Bernard, B.F., Visser, T.J., Bakker, W.H., Breeman, W.A., Krenning, E.P., 1996. Inhibition of renal uptake of indium-111-DTPA-octreotide in vivo. J. Nucl. Med. 37, 1388–1392.

De Vincentis, G., Remediani, S., Varvarigou, A.D., Di Santo, G., Iori, F., Laurenti, C., Scopinaro, F., 2004. Role of ^{99m}Tc-bombesin scan in diagnosis and staging of prostate cancer. Cancer Biother. Radiopharm. 19 (1), 81–84.

de Visser, M., Bernard, H.F., Erion, J.L., Schmidt, M.A., Srinivasan, A., Waser, B., Reubi, J.C., Krenning, E.P., de Jong, M., 2007. Novel ^{111}In-labelled bombesin analogues for molecular imaging of prostate tumors. Eur. J. Nucl. Med. Mol. Imag. 34, 1228–1238.

de Visser, M., Verwijnen, S.M., de Jong, M., 2008. Update: improvement strategies for peptide receptor scintigraphy and radionuclide therapy. Cancer Biother. Radiopharm. 23 (2), 137–157.

Nstoforo, C., Mather, S.J., 2002. The influence of chelator on the pharmacokinetics of ^{99m}Tc-labelled peptides. Q. J. Nucl. Med. 46, 195–205.

Fragogeorgi, E.A., Zikos, C., Gourni, E., Bouziotis, P., Paravatou-Petsotas, M., Loudos, G., Mitsokapas, N., Xanthopoulos, S., Mavri-Vavayanni, M., Livaniou, E., Varvarigou, A.D., Archimandritis, S.C., 2009. Spacer site modifications for the improvement of the in vitro and in vivo binding properties of ^{99m}Tc-N$_3$S-X-Bombesin[2-14] derivatives. Bioconjug. Chem. 20, 856–867.

Garayoa, E.G., Schweinsberg, C., Maes, V., Brans, L., Blauenstein, P., Tourwe, D.A., Beck-Sickinger, A.G., Schibli, R., Schubiger, P.A., 2008. Influence of the molecular charge on the biodistribution of bombesin analogues labelled with the [^{99m}Tc(CO)$_3$-Core]. Bioconjugate Chem. 19 (12), 2409–2416.

Garayoa, E.G., Ruegg, D., Blauenstein, P., Zwimpfer, M., Khan, I.A., Maes, V., Blanc, A., Beck-Sickinger, A., Tourwe, A.G., Schubiger, P.A., 2007. Chemical and biological characterization of new Re(CO)$_3$/^{99m}Tc(CO)$_3$ bombesin analogues. Nucl. Med. Biol. 34, 17–28.

Giblin, M.F., Veerendra, B., Smith, C.J., 2005. Radiometallation of Receptor-specific peptides for diagnosis and treatment of human cancer. In Vivo 19, 9–30.

Gotthardt, M., van Eerd-Vismale, J., Oyen, W.J., de Jong, M., Zhang, H., Rolleman, E., Maecke, H.R., Béhé, M., Boerman, O., 2007. Indication for different mechanisms of kidney uptake of radiolabelled peptides. J. Nucl. Med. Apr. 48 (4), 596–601.

Gourni, E., Bouziotis, P., Benaki, D., Loudos, G., Xanthopoulos, S., Paravatou-Petsotas, M., Mavri-Vavagianni, M., Pelecanou, M., Archimandritis, S.C., Varvarigou, A.D., 2009. Structural assessment and biological evaluation of two N3S bombesin derivatives. J. Med. Chem. 52 (14), 4234–4246.

Gu, D., Ma, Y., Niu, G., Yan, Y., Lang, L., Akber Aisaand, H., Gao, H., Kiesewetter, D.O., Chen, X., 2011. LC/MS evaluation of metabolism and membrane transport of bombesin peptides. Amino Acids 40 (2), 669–675.

IAEA-TECDOC-1214, 1995–1999. ^{99m}Tc labelled peptides for imaging of peripheral receptors. Final report of a co-ordinated research project.

Jankowsky, R., Kirsch, S., Reich, T., Spies, H., Johannsen, B., 1998. Solution structures of rhenium(V) oxo peptide complexes of glycylglycylcysteine and cysteinylglycine as studied by capillary electrophoresis and X-ray absorption spectroscopy. J. Inorg. Biochem. 70, 99–106.

Jensen, R.T., Battey, J.F., Spindel, E.R., Benya, R.V., 2008. International Union of Pharmacology. LXVIII. Mammalian bombesin receptors: nomenclature, distribution, pharmacology, signaling, and functions in normal and disease states. Pharmacol. Rev. 60, 1–42.

Kimmerlin, T., Seebach, D., 2005. '100 years of peptide synthesis': ligation methods for peptide and protein synthesis with applications to b-peptide assemblies. J. Peptide Res. 65, 229–260.

Kolenc-Peitl, P., Mansi, R., Tamma, M., Gmeiner-Stopar, T., Sollner-Dolenc, M., Waser, B., Baum, R.P., Reubi, J.C., Maecke, H.R., 2011. Highly improved metabolic stability and pharmacokinetics of indium-111-DOTA-gastrin conjugates for targeting of the gastrin receptor. J. Med. Chem. 54, 2602–2609.

Kunstler, J.U., Veerendra, B., Figueroa, S.D., Sieckman, G.L., Rold, T.L., Hoffman, T.J., Smith, L.C.J., Pietzsch, H.J., 2007. Organometalic ^{99m}Tc(III) '4+1' Bombesin(7–14) conjugates: synthesis, radiolabelling, and in vitro/in vivo studies. Bioconjugate Chem. 18, 1651–1661.

La Bella, R., Garcia-Garayoa, E., Larger, M., Bläuenstein, P., Beck-Sickinger, A.G., Schubiger, P.A., 2002a. *In vitro* and *in vivo* evaluation of a ^{99m}Tc(I)-labelled bombesin analogue for imaging of gastrin releasing peptide receptor-positive tumors. Nucl. Med. Biol. 29, 553–560.

La Bella, R., Garcia-Garayoa, E., Bähler, M., Bläuenstein, P., Schibli, R., Conrath, P., Tourwé, D., Schubiger, P.A., 2002b. A ^{99m}Tc(I)-postlabelled high affinity bombesin analogue as a potential tumor imaging agent. Bioconjugate Chem. 13, 599–604.

Lane, S.R., Veerendra, B., Rold, T.L., Sieckman, G.L., Hoffman, T.J., Jurisson, S.S., Smith, C.J., 2008. ^{99m}Tc(CO)$_3$-DTMA bombesin conjugates having high affinity for the GRP receptor. Nucl. Med. Biol. 35, 263–272.

Lane, S.R., Nanda, P., Rold, T.L., Sieckman, G.L., Figueroa, S.D., Hoffman, T.J., Jurisson, S.S., Smith, C.J., 2010. Optimization, biological evaluation and microPET imaging of copper-64-labelled bombesin agonists, [^{64}Cu-NO2A-(X)-BBN(7-14)NH$_2$], in a prostate tumor xenografted mouse model. Nucl. Med. Biol. 37, 751–761.

Lantry, L.E., Cappelletti, E., Maddalena, M.E., Fox, J.S., Feng, W., Chen, J., Thomas, R., Eaton, S.M., Bogdan, N.J., Arunachalam, T., Reubi, J.C., Raju, N., Metcalfe, E.C., Lattuada, L., Linder, K.E., Swenson, R.E., Tweedle, M.F., Nunn, A.D., 2006. ^{177}Lu-AMBA: synthesis and characterization of a selective 177Lu-labelled GRP-R agonist for systemic radiotherapy of prostate cancer. J. Nucl. Med. 47, 1144–1152.

Lee, S., Xie, J., Chen, X., 2010. Peptides and peptide hormones for molecular imaging and disease diagnosis. Chem. Rev. 110, 3087–3111.

Lin, K.-S., Luu, A., Baidoo, K.E., Hashemzadeh-Gargari, H., Chen, M.-K., Pili, R., Pomper, M., Carducci, M., Wagner Jr., H.N., 2004. A new high affinity technetium analogue of bombesin containing DTPA as a pharmacokinetic modifier. Bioconjugate Chem. 15, 1416–1423.

Lin, K.-S., Luu, A., Baidoo, K.E., Hashemzadeh-Gargari, H., Chen, M.-K., Brenneman, K., Pili, R., Pomper, M., Carducci, M.A., Wagner Jr., H.N., 2005. A new high affinity technetium-99m-bombesin analogue with low abdominal accumulation. Bioconjugate Chem. 16, 43–50.

Linder, K.E., Metcalfe, E., Arunachalam, T., Chen, J., Eaton, S.M., Feng, W., Fan, H., Raju, N., Cagnolini, A., Lantry, L.E., Nunn, A.D., Swenson, R.E., 2009. In vitro and in vivo metabolism of Lu-AMBA, a GRP-receptor binding compound, and the synthesis and characterization of its metabolites. Bioconjugate Chem. 20 (6), 1171–1178.

Lister-James, J., Moyer, B.R., Dean, T., 1996. Small peptides radiolabelled with ^{99m}Tc. Q. J. Nucl. Med. 40, 221–233.

Liu, S., Edwards, D.S., 1999. ^{99m}Tc-labelled small peptides as diagnostic radiopharmaceuticals. Chem. Rev. 99, 2235–2268.

Loudos, G., Majewski, S., Wojcik, R., Weisenberger, A., Sakellios, N., Nikita, K., Uzunoglu, N., Bouziotis, P., Xanthopoulos, St., Varvarigou, A., 2007. Performance evaluation of a dedicated camera suitable for dynamic radiopharmaceuticals evaluation in small animals. IEEE Trans. Nucl. Sci. 54 (3), 454–460.

Mantey, S., Frucht, H., Coy, D.H., Jensen, R.T., 1993. Characterization of bombesin receptors using a novel, potent, radiolabelled antagonist that distinguishes bombesin receptor subtypes. Mol. Pharmacol. 43, 762–774.

Nanda, P.K., Lane, S.R., Retzloff, L.B., Pandey, U.S., Smith, C.J., 2010. Radiolabelled regulatory peptides for imaging and therapy. Curr. Opin. Endocrinol. Diabetes Obes. 17 (1), 69–76.

Noll, B., Kniess, T., Friebe, M., Spies, H., Johannsen, B., 1996. Rhenium $^{(V)}$ gluconate, a suitable precursor for the preparation of Rhenium$^{(V)}$ complexes. Isotopes Environ. Health Stud. 32, 21–29.

Okarvi, S.M., 2004. Peptide-based radiopharmaceuticals: future tools for diagnostic imaging of cancers and other diseases. Med. Res. Rev. 24 (5), 685–686.

Parry, J.J., Kelly, T.S., Andrews, R., Rogers, B.E., 2007. In vitro and in vivo evaluation of ^{64}Cu-labelled DOTA-linker-Bombesin(7-14) analogues containing different amino acid spacer moieties. Bioconjugate Chem. 18 (4), 1110–1117.

Prasanphanich, A.F., Lane, S.R., Figueroa, S.D., Ma, L., Rold, T.L., Sieckman, G.L., Hoffman, T.J., McCrate, J.M., Smith, C.J., 2007. The effects of linking substituents on the in vivo behavior of site-directed, peptide-based diagnostic radiopharmaceuticals. In Vivo 21 (1), 1–16.

Reubi, J.C., 2003. Peptide receptors as molecular targets for cancer diagnosis and therapy. Endocr. Rev. 24 (4), 389–427.

Rogers, B.E., Bigott, H.M., McCarthy, D.W., Della Manna, D., Kim, J., Sharp, T.L., Welch, M.J., 2003. MicroPET imaging of a gastrin-releasing peptide receptor-positive tumor in a mouse model of human prostate cancer using a ^{64}Cu-labelled bombesin analogue. Bioconjugate Chem. 14, 756–763.

Rogers, B.E., Rosenfeld, M.E., Khazaeli, M.B., Mikheeva, G., Stackhouse, M.A., Liu, T., Curiel, D.T., Buchsbaum, D.J., 1997. Localization of iodine-125-mIP-Des-Met14-bombesin (7-13)NH_2 in ovarian carcinoma induced to express the gastrin releasing peptide receptor by adenoviral vector-mediated gene transfer. J. Nucl. Med. 38 (8), 1221–1229.

Rolleman, E.J., Valkema, R., de Jong, M., Kooij, P.P., Krenning, E.P., 2003. Safe and effective inhibition of renal uptake of radiolabelled octreotide by a combination of lysine and arginine. Eur. J. Nucl. Med. Mol. Imaging 30, 9–15.

Sarin, V.K., Kent, S.B.H., Tam, J.P., Merrifield, R.B., 1981. Quantitative monitoring of solid phase peptide synthesis by the ninhydrin reaction. Anal. Biochem. 117, 147–157.

Schweinsberg, C., Maes, V., Brans, L., Bläuenstein, P., Tourwé, D.A., Schubiger, P.A., Schibli, R., García Garayoa, E., 2008. Novel glycated [^{99m}Tc(CO)$_3$]-labelled bombesin analogues for improved targeting of gastrin-releasing peptide receptor-positive tumors. Bioconjugate Chem. 19 (12), 2432–2439.

Scopinaro, F., De Vincentis, G., Varvarigou, A.D., Laurenti, C., Iori, F., Remediani, S., Chiarini, S., Stella, S., 2003. ^{99m}Tc-bombesin detects prostate cancer and invasion of pelvic lymph nodes. Eur. J. Nucl. Med. Mol. Imaging 30, 1378–1382.

Scopinaro, F., De Vincentis, G., Corazziari, E., Massa, R., Osti, M., Pallotta, N., Covotta, A., Remediani, S., Di Paolo, M., Monteleone, F., Varvarigou, A., 2004. Detection of colon cancer with ^{99m}Tc-labelled bombesin derivative (^{99m}Tc-leu13-BN1). Cancer Biother. Radiopharm. 19 (2), 245–252.

Seo, Y., Kurhanewicz, J., Franc, B.L., Hawkins, R.A., Hasegawa, B.H., 2005. Improved prostate cancer imaging with SPECT/CT and MRI/MRSI. IEEE Trans. Nucl. Sci. 52 (5), 1316–1320.

Shipp, M.A., Tarr, G.E., Chen, C.-Y., Switzer, S.N., Hersh, L.B., Stein, H., Sunday, M.E., Reinherz, E.L., 1991. CD10/neutral endopeptidase 24.11 hydrolyzes bombesin-like peptides and regulates the growth of small cell carcinomas of the lung. Proc. Natl. Acad. Sci. U. S. A. Cell Biol. 88, 10662–10666.

Smith, C.J., Gali, H., Sieckman, G.L., Higginbotham, C., Volkert, W.A., Hoffman, T.J., 2003a. Radiochemical investigations of ^{99m}Tc–N_3S-X-BBN[7–14]NH_2: an in vitro/in vivo structure–activity relationship study where *X* = 0-, 3-, 5-, 8-, and 11-carbon tethering moieties. Bioconjugate Chem. 14 (1), 93–102.

Smith, C.J., Sieckman, G.L., Owen, N.K., Hayes, D.H., Mazuru, D.G., Kanna, R., Volkert, W.A., Hoffman, T.J., 2003b. Radiochemical investigations of gastrin-releasing peptide receptor specific [^{99m}Tc(X)(CO_3)-Dpr-Ser-Ser-Ser-Gln-Trp-Ala-Val-Gly-His-Leu-Met-(NH_2)] in PC-3, tumor-bearing, rodent models: syntheses, Radiolabelling and in vitro/vivo studies where Dpr = 2,3-Diaminopropionic acid and X = H_2O or P(CH_2OH)$_3$. Cancer Res. 63, 4082–4088.

Smith, C.J., Volkert, W.A., Hoffman, T.J., 2005. Radiolabelled peptide conjugates for targeting of the bombesin receptor superfamily subtypes. Nucl. Med. Biol. 32, 733–740.

Spindel, E.R., 2003. Bombesin-like peptides. In: Henry, H.L., Norman, A.W. (Eds.), Encyclopedia of Hormones. Elsevier–Academic Press, pp. 198–205.

Trejtnar, F., Laznicek, M., Laznickova, A., Mather, S.J., 2000. Pharmacokinetics and renal handling of ^{99m}Tc-labelled peptides. J. Nucl. Med. 41 (1), 177–182.

Van de Wiele, C., Dumont, F., Broecke, R.V., Oosterlinck, W., Cocquyt, V., Serreyn, R., Peers, S., Thornback, J., Slegers, G., Dierckx, R.A., 2000. Technetium-99m RP527, a GRP analogue for visualisation of GRP receptor-expressing malignancies: a feasibility study. Eur. J. Nucl. Med. 27, 1694–1699.

Van de Wiele, C., Dumont, F., Van Belle, S., Slegers, G., Peers, S.H., Dierckx, R.A., 2001a. Is there a role for agonist gastrin-releasing peptide receptor radioligands in tumor imaging? Nucl. Med. Commun. 22, 5–15.

Van de Wiele, C., Dumont, F., Dierckx, R.A., Peers, S.H., Thornback, J.R., Slegers, G., Thierens, H., 2001b. Biodistribution and dosimetry of ^{99m}Tc-RP527, a gastrin-releasing peptide (GRP) agonist for the visualization of GRP receptor–expressing malignancies. J. Nucl. Med. 42 (11), 1722–1727.

Van de Wiele, C., Phonteyne, P., Pauwels, P., Goethals, I., Van Den Broecke, R., Cocquyt, V., Dierckx, R.A., 2008. Gastrin-releasing peptide receptor imaging in human breast carcinoma versus immunohistochemistry. J. Nucl. Med. 49 (2), 260–264.

Veerendra, B., Sieckman, G.L., Hoffman, T.J., Rold, T., Retzloff, L., McCrate, J., Prasanphanich, A., Smith, C.J., 2006. Synthesis, radiolabelling and in vitro GRP receptor targeting studies of ^{99m}Tc-Triaza-X-BBN[7-14]NH_2 (X = Serylserylserine, Glycylglycylglycine, Glycylserylglycine, or Beta Alanine). Synth. React. Inorg. M. 36, 481–491.

Wong, E., Fauconnier, T., Bennett, S., Valliant, J., Nguyen, T., Lau, F., Lu, L.F.L., Pollak, A., Bell, R.A., Thornback, J.R., 1997. Rhenium (V) and technetium (V) oxo complexes of an N_2NS peptidic chelator: evidence of interconversion between the syn and anti conformations. Inorg. Chem. 36, 5799–5808.

Yang, Y.-S., Zhang, X., Xiong, Z., Chen, X., 2006. Comparative in vitro and in vivo evaluation of two ^{64}Cu-labelled bombesin analogs in a mouse model of human prostate adenocarcinoma. Nucl. Med. Biol. 33 (3), 371–380.